

Berry Phases of Vison Transport in \mathbb{Z}_2 Topologically Ordered States from Exact Fermion-Flux Lattice Dualities

Chuan Chen,^{1,2} Peng Rao,² and Inti Sodemann^{2,3,*}

¹*Institute for Advanced Study, Tsinghua University, 100084 Beijing, China*

²*Max-Planck Institute for the Physics of Complex Systems, 01187 Dresden, Germany*

³*Institut für Theoretische Physik, Universität Leipzig, 04103 Leipzig, Germany*

(Dated: October 12, 2022)

We develop an exact map of all states and operators from 2D lattices of spins-1/2 into lattices of fermions and bosons with mutual semionic statistical interaction that goes beyond previous dualities of \mathbb{Z}_2 lattice gauge theories because it does not rely on imposing local conservation laws and captures the motion of “charges” and “fluxes” on equal footing. This map allows to explicitly compute the Berry phases for the transport of fluxes in a large class of symmetry enriched topologically ordered states with emergent \mathbb{Z}_2 gauge fields that includes chiral, non-chiral, abelian or non-abelian, that can be perturbatively connected to models where the visons are static and the emergent fermionic spinons have a non-interacting dispersion. The numerical complexity of computing such vison phases reduces therefore to computing overlaps of ground states of free-fermion Hamiltonians. Among other results, we establish numerically the conditions under which the Majorana-carrying flux excitation in Ising-Topologically-Ordered states enriched by translations acquires 0 or π phase when moving around a single plaquette.

I. INTRODUCTION

One of the best understood families of spin liquids are those featuring emergent \mathbb{Z}_2 gauge fields [1, 2]. These spin liquids, which include the original Anderson short-ranged RVB state [3, 4], feature a non-local fermion (spinon) and a “ π -flux” (vison) excitation [5–8]. Kitaev’s toric code (TC) [9] is perhaps the simplest exactly solvable model for these kind of spin liquids. A recent series of works [10–12] have shown that, beyond being an exactly solvable model, the TC offers a new way to organize the Hilbert space. In Ref. [10], it has been shown that by imposing a new type of local \mathbb{Z}_2 constraint (local symmetry) on a spin model, the local gauge invariant spin operators can be exactly mapped onto local fermion bilinears. This construction can be viewed as a generalization of the procedure that allows to solve the Kitaev honeycomb model exactly [13], where the \mathbb{Z}_2 constraint immobilizes the flux excitations leaving the fermions as the only dynamical objects of the problem. For related constructions see Refs. [13–18]. The construction of Ref. [10] provides a local map from fermion bilinear operators onto spin operators in 2D, and it serves to rewrite in an exact manner any imaginable local Hamiltonian of fermions as a local Hamiltonian of spins restricted to a subspace satisfying the \mathbb{Z}_2 local conservation laws. Thus, for example, any free fermion model can be obtained as an exact description of a subspace of the Hamiltonian of a spin model.

In this work we extend the mapping of Ref. [10] by constructing an exact lattice duality mapping of the *full* Hilbert space of the underlying spins onto a dual space of spinons and visons *without* imposing any local \mathbb{Z}_2 conservation laws that would freeze the motion of these par-

ticles. Namely, we will construct non-local spinon and vison creation/annihilation operators in a completely explicit form in terms of underlying spin-1/2 operators. One of the key properties of our construction is that the dual Hilbert space completely “disentangles” the vison and emergent fermion degrees of freedom, in the sense that the dual states can be organized as tensor products of vison and emergent fermion configurations. We will use this construction to compute the Berry phases associated with transporting the vison around plaquettes in closed loops in the background of topological superconducting state of the spinons with a non-zero Chern number. Throughout this work we will refer to the vison π -flux excitations sometimes as “ e -particles” and the fermionic spinons as the “ ε -particles”. A recent work [12] computed these phases when the fermions were in BdG states with zero Chern number, relying on the property that these could be realized as ground states of commuting projector Hamiltonians. But it is known that chiral states cannot be realized in this fashion [19], and therefore our current approach overcomes these limitations.

The rest of the paper is organized as follows: Sec. II contains the theoretical foundation of this work, which is an exact duality mapping of a 2D spin system and a Hilbert space of mutual semions. In Sec. II A, we introduce the duality mapping where the dual space consists of e (boson) and m (boson) particles; in Sec. II B, we introduce the mapping with the dual space containing visons (e boson) and spinons (ε fermion). As an application of this new theoretical tool, we computed the vison Berry phases for the celebrated Kitaev model. The model (and its dual form) was briefly reviewed in Sec. III. Our main results are presented in Sec. IV: Sec. IV A shows the results for the Kitaev model with a finite spinon Haldane mass term, and the results for a model with a higher spinon Chern number ($C = -2$) are presented in Sec. IV B. We summarize and discuss our findings in

* sodemann@itp.uni-leipzig.de

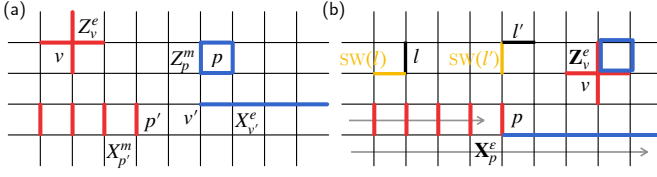


FIG. 1. Schematic of the infinite system for both boson-boson and boson-fermion mappings. (a) Operators for the boson-boson mapping (infinite lattice). Spin X (Z) operators at each link are represented by red (blue) colored bonds. (b) Operators for the boson-fermion mapping (infinite lattice). The gray arrow indicates the sequence of plaquettes in the Jordan-Wigner transformation, which increases from lower to upper rows.

Sec. V.

II. DUALITY MAPPING

A. Boson-boson mapping

In this section, we will illustrate the idea of the boson-boson mapping. For simplicity, here we will focus on the case of an *infinite* system, the mappings on an open and a periodic system are provided in the Supplementary Information [20].

As has been shown explicitly in the TC model [9], for a 2D spin system with spins residing on the links of a square lattice (its Hilbert space will be denoted as $\mathcal{H}_{\text{spin}}$), one can define the so-called star and plaquette operators associated with each vertex and plaquette respectively:

$$A_v = \prod_{l \in \text{star}(v)} X_l, \quad B_p = \prod_{l \in \text{boundary}(p)} Z_l. \quad (1)$$

All the A_v and B_p commute with each other, moreover, the eigenstates of them form a basis of the spin Hilbert space $\mathcal{H}_{\text{spin}}$. One can define a dual spin system $\mathcal{H}_{e\text{-spin}} \times \mathcal{H}_{m\text{-spin}}$ containing two types of *spins*, denoted as e and m spins. Here the e and m spins sit on the vertices and plaquettes of the square lattice respectively, whose spin Z configurations are related to the occupation of the e and m particles (see below). The local spin X and Z Pauli matrices of the dual e (m) spins are denoted as X_v^e (X_p^m) and Z_v^e (Z_p^m), which satisfy the following commutation relations:

$$[X_v^e, Z_{v'}^e] = 0 \quad (v \neq v'), \quad \{X_v^e, Z_v^e\} = 0, \quad (2a)$$

$$[Z_p^m, X_{p'}^m] = 0 \quad (p \neq p'), \quad \{Z_p^m, X_p^m\} = 0, \quad (2b)$$

$$[X_v^e, X_p^m] = [Z_v^e, Z_p^m] = [X_v^e, Z_p^m] = [Z_v^e, X_p^m] = 0. \quad (2c)$$

Within the duality mapping, we shall map the eigenbasis of A_v and B_p from $\mathcal{H}_{\text{spin}}$ to the local spin Z eigenbasis of e and m spins, such that the star and plaquette operators are mapped to the spin Z Pauli matrices of e and m spins respectively:

$$A_v \leftrightarrow Z_v^e, \quad B_p \leftrightarrow Z_p^m. \quad (3)$$

To make the dual operators of X_v^e , Z_v^e , X_p^m and Z_p^m should also satisfy the algebraic relations in Eq. (2), we found that the following choice of dual operators do the job:

$$\prod_{l \in R(v)} Z_l \leftrightarrow X_v^e, \quad \prod_{l \in L(p)} X_l \leftrightarrow X_p^m. \quad (4)$$

Here $R(v)$ stands for the horizontal links to the right of vertex v , $L(p)$ stands for the vertical links to the left of plaquette p (see Fig. 1(a) for a schematic of the non-local operators above). It can be shown that the local spin X and Z operators in $\mathcal{H}_{\text{spin}}$ can be mapped to:

i). Vertical l :

$$X_l \leftrightarrow X_{p_1}^m X_{p_2}^m, \quad Z_l \leftrightarrow X_{v_1}^e X_{v_2}^e \prod_{p \in R(l)} Z_p^m. \quad (5)$$

ii). Horizontal l :

$$X_l \leftrightarrow X_{p_1}^m X_{p_2}^m \prod_{v \in L(l)} Z_v^e, \quad Z_l \leftrightarrow X_{v_1}^e X_{v_2}^e. \quad (6)$$

Here for any vertical (horizontal) link l , the two vertices connected by it are denoted as v_1 and v_2 , the plaquettes to its left (top) and right (bottom) are called p_1 and p_2 . $L(l)$ stands for vertices to the left of a horizontal l (including v_1). Note that spin X_l and Z_l operators form a complete algebraic basis out of which any other spin operators can be written in terms of their summation, products and multiplication with complex numbers. In this way, we have established the duality mapping between $\mathcal{H}_{\text{spin}}$ and $\mathcal{H}_{e\text{-spin}} \times \mathcal{H}_{m\text{-spin}}$.

Since spin-1/2 degrees of freedom can be equivalently viewed as hard-core (e and m) bosons, it is straightforward to establish the mapping $\mathcal{H}_{e\text{-spin}} \times \mathcal{H}_{m\text{-spin}} \leftrightarrow \mathcal{H}_e \times \mathcal{H}_m$, the e and m spins' Pauli matrices can be written as bosonic operators:

$$Z_v^e \leftrightarrow (-1)^{b_v^\dagger b_v}, \quad X_v^e \leftrightarrow (b_v + b_v^\dagger), \quad (7a)$$

$$Z_p^m \leftrightarrow (-1)^{d_p^\dagger d_p}, \quad X_p^m \leftrightarrow (d_p + d_p^\dagger). \quad (7b)$$

Here b_v (d_p) is the annihilation operator of an e (m) boson at vertex v (plaquette p).

Finally, we obtain the duality mapping between $\mathcal{H}_{\text{spin}}$ and $\mathcal{H}_e \times \mathcal{H}_m$, where the star and plaquettes operators of the original spin space are mapped to the parity operators of e and m bosons:

$$A_v \leftrightarrow (-1)^{b_v^\dagger b_v}, \quad B_p \leftrightarrow (-1)^{d_p^\dagger d_p}. \quad (8)$$

The local spin operators are mapped into:

i). Vertical l :

$$X_l \leftrightarrow (d_{p_1} + d_{p_1}^\dagger)(d_{p_2} + d_{p_2}^\dagger), \quad (9)$$

$$Z_l \leftrightarrow (b_{v_1} + b_{v_1}^\dagger)(b_{v_2} + b_{v_2}^\dagger) \prod_{p \in R(l)} (-1)^{d_p^\dagger d_p}. \quad (10)$$

ii). Horizontal l :

$$X_l \leftrightarrow \prod_{v \in L(l)} (-1)^{b_v^\dagger b_v} (d_{p_1} + d_{p_1}^\dagger)(d_{p_2} + d_{p_2}^\dagger), \quad (11)$$

$$Z_l \leftrightarrow (b_{v_1} + b_{v_1}^\dagger)(b_{v_2} + b_{v_2}^\dagger). \quad (12)$$

Within this duality mapping, local Z_l (X_l) operators have the effect of pair fluctuating and hopping the e (m) particles on nearest-neighbor vertices v_1 and v_2 (plaquettes p_1 and p_2), as one would naturally expect since they anti-commute with the e (m) particles' parity operator at those two vertices (plaquettes). More interestingly, there is also a product of m (e) particles' parity operators when the e (m) particle is hopping along y -direction [21], such non-local statistical interaction terms make the e and m particles mutual semions.

B. Boson-fermion mapping

1. Infinite lattice

It turns out that it is also possible to map the $\mathcal{H}_{\text{spin}}$ to a space of bosons (e particles) and fermions (ε particles), $\mathcal{H}_e \times \mathcal{H}_\varepsilon$. For pedagogical reason, we will start with the case with an infinite lattice, and introduce the mapping on a periodic system in the next section. The mapping for an open lattice can be found in the Supplementary information [20].

Each ε particle in the boson-fermion mapping can be viewed as a composite of an e and an m particles of the boson-boson mapping, and the e and ε particles are mutual semions [9]. Same as the boson-boson mapping introduced in the previous section, the mapping between $\mathcal{H}_{\text{spin}}$ and $\mathcal{H}_e \times \mathcal{H}_\varepsilon$ can be made more obvious if one first introduces an intermediate dual spin space $\mathcal{H}_{e\text{-spin}} \times \mathcal{H}_{\varepsilon\text{-spin}}$, where the e (ε) spins are located at the vertices (plaquettes) of a square lattice. Recall that the eigenstates of A_v and B_p are also eigenstates of all the $A_v B_{p(v)}$ and B_p . Here $p(v)$ stands for the plaquettes to the northeast of vertex v . One can map this eigenbasis to the local spin Z eigenbasis of e and ε spins of the intermediate dual space, such that

$$A_v B_{p(v)} \leftrightarrow \mathbf{Z}_v^e, B_p \leftrightarrow \mathbf{Z}_p^\varepsilon. \quad (13)$$

Note that here we used bold symbols to denote the Pauli matrices of the e and ε spins, which satisfy the following algebraic relations:

$$[\mathbf{X}_v^e, \mathbf{Z}_{v'}^e] = 0 \ (v \neq v'), \ \{\mathbf{X}_v^e, \mathbf{Z}_v^e\} = 0, \quad (14a)$$

$$[\mathbf{Z}_p^\varepsilon, \mathbf{X}_{p'}^\varepsilon] = 0 \ (p \neq p'), \ \{\mathbf{Z}_p^\varepsilon, \mathbf{X}_p^\varepsilon\} = 0, \quad (14b)$$

$$[\mathbf{Z}_v^e, \mathbf{Z}_p^\varepsilon] = [\mathbf{X}_v^e, \mathbf{X}_p^\varepsilon] = [\mathbf{X}_v^e, \mathbf{Z}_p^\varepsilon] = [\mathbf{Z}_v^e, \mathbf{X}_p^\varepsilon] = 0. \quad (14c)$$

In $\mathcal{H}_{\text{spin}}$, the dual operators of \mathbf{X}_v^e and \mathbf{X}_p^ε will respect

these relations if one choose:

$$\prod_{l \in R(v)} Z_l \leftrightarrow \mathbf{X}_v^e, \quad (15)$$

$$\prod_{l \in R(v(p))} Z_l \prod_{l' \in L(p)} X_{l'} \leftrightarrow \mathbf{X}_p^\varepsilon. \quad (16)$$

Here $v(p)$ stands for the vertex to the southwest of plaquette p . A schematic of these non-local spin operators are shown in Fig. 1(b). In this way, we have completed the mapping between $\mathcal{H}_{\text{spin}}$ and $\mathcal{H}_{e\text{-spin}} \times \mathcal{H}_{\varepsilon\text{-spin}}$.

The mapping from $\mathcal{H}_{e\text{-spin}} \times \mathcal{H}_{\varepsilon\text{-spin}}$ to $\mathcal{H}_e \times \mathcal{H}_\varepsilon$ is more straightforward, the e particles is just the hard-core boson corresponding to the e spins, and the $\mathcal{H}_{\varepsilon\text{-spin}}$ is mapped to \mathcal{H}_ε through a Jordan-Wigner transformation:

$$\mathbf{Z}_v^e \leftrightarrow (-1)^{b_v^\dagger b_v}, \ \mathbf{X}_v^e \leftrightarrow (b_v + b_v^\dagger), \quad (17)$$

$$\mathbf{Z}_p^\varepsilon \leftrightarrow -i\gamma_p \gamma_p', \ \mathbf{X}_p^\varepsilon \leftrightarrow \left(\prod_{q < p} -i\gamma_q \gamma_q' \right) \gamma_p'. \quad (18)$$

Here b_v (b_v^\dagger) is the annihilation (creation) operator for the e particle at vertex v . We have also introduced two Majorana fermion modes (γ_p and γ_p') to represent the complex ε fermion mode (whose annihilation/creation operator is c_p/c_p^\dagger) at each plaquette p , with

$$\gamma_p = c_p + c_p^\dagger, \ \gamma_p' = \frac{1}{i}(c_p - c_p^\dagger). \quad (19)$$

Note that the fermion parity at each plaquette p is $(-1)^{c_p^\dagger c_p} = -i\gamma_p \gamma_p'$. The sequence of plaquettes in the Jordan-Wigner transformation is indicated by the gray arrow in Fig. 1(b). In this way, we have established the mapping between $\mathcal{H}_{\text{spin}}$ and $\mathcal{H}_e \times \mathcal{H}_\varepsilon$, it can be shown that the following local spin operators are mapped to:

i). l is a vertical link:

$$X_l Z_{\text{SW}(l)} \leftrightarrow \mathbf{X}_{p_1}^\varepsilon \mathbf{X}_{p_2}^\varepsilon \leftrightarrow i\gamma_{p_1} \gamma_{p_2}', \quad (20)$$

$$Z_l \leftrightarrow \mathbf{X}_{v_1}^e \mathbf{X}_{v_2}^e \prod_{p \in R(l)} \mathbf{Z}_p^\varepsilon \leftrightarrow (b_{v_1} + b_{v_1}^\dagger)(b_{v_2} + b_{v_2}^\dagger) \prod_{p \in R(l)} (-i\gamma_p \gamma_p'). \quad (21)$$

ii). l is a horizontal link:

$$X_l Z_{\text{SW}(l)} \leftrightarrow (-1) \prod_{v \in L(l)} \mathbf{Z}_v^e \left(\prod_{p_2 \leq p \leq p_1} \mathbf{Z}_p^\varepsilon \right) \mathbf{X}_{p_1}^\varepsilon \mathbf{X}_{p_2}^\varepsilon \leftrightarrow \prod_{v \in L(l)} (-1)^{b_v^\dagger b_v} i\gamma_{p_1} \gamma_{p_2}' \quad (22)$$

$$Z_l \leftrightarrow \mathbf{X}_{v_1}^e \mathbf{X}_{v_2}^e \leftrightarrow (b_{v_1} + b_{v_1}^\dagger)(b_{v_2} + b_{v_2}^\dagger). \quad (23)$$

Here $\text{SW}(l)$ is the link to the southwest of link l , which also connects to it (see Fig. 1(b) for a schematic). It is

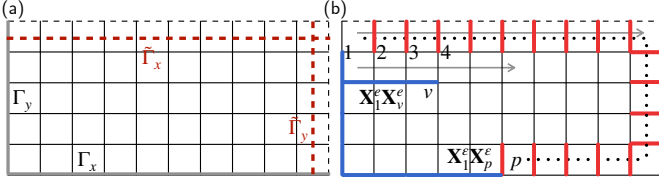


FIG. 2. Schematic of operators in the boson-fermion mapping for a periodic lattice. (a) Non-contractible loops used in the definition of Wilson loop and t'Hooft operators. $\Gamma_{x/y}$ is highlighted in gray color and $\tilde{\Gamma}_{x/y}$ is highlighted in red color. (b) The dual of $\mathbf{X}_1^e \mathbf{X}_v^e$ and $\mathbf{X}_1^e \mathbf{X}_p^e$ operators. The sequence of vertices and the associated plaquettes (to the northeast of each vertex) starts with the one on the top left, ascends towards the right direction within each row and increases from the top to bottom rows, as indicated by the gray arrow. The $\Gamma_{1,v}$ path starts from vertex 1, goes down first then goes to the right direction until reaching vertex v , see the path paved by blue coloured bonds. The dual path $\tilde{\Gamma}_{1,p}$ starts from plaquette 1, goes to the right end first, then goes down, and finally goes left until plaquette p . An example is indicated by the black dotted line in the figure.

clear that the local Z_l ($X_l Z_{\text{SW}}(l)$) operator is able to pair create, annihilate and hop the e (ε) particles in the nearest neighbors. The non-local products of the e -particle (ε -particle) parities in the dual operator of $X_l Z_{\text{SW}}(l)$ (Z_l) indicates the statistical interaction between e and ε particles, which view each other as π fluxes, i.e., they are mutual semions.

2. Periodic lattice

The idea of the duality mapping on a periodic lattice (torus) is basically the same as the infinite lattice case. However, there are now two global constraints in the original spin space:

$$\prod_v A_v B_{p(v)} = 1, \quad \prod_p B_p = 1. \quad (24)$$

Therefore, only an even number of $A_v B_{p(v)}$ and B_p can take -1 , i.e., there are only 2^{2N-2} different configurations of $A_v B_{p(v)}$ and B_p , where N is the number of unit cells in the system. To fully characterize the spin Hilbert space (with dimension 2^{2N}), one needs to introduce two additional Wilson loop degrees of freedom. The Wilson loop operators commutes with all the $A_v B_{p(v)}$ and B_p operators, one possible choice is:

$$W_1 = - \prod_{l \times \tilde{\Gamma}_x} X_l \prod_{l' \in \Gamma_x} Z_{l'}, \quad W_2 = - \prod_{l \times \tilde{\Gamma}_y} X_l \prod_{l' \in \Gamma_y} Z_{l'}. \quad (25)$$

Here $l \times \tilde{\Gamma}_{x/y}$ denotes the link l crossing the dual-lattice path $\tilde{\Gamma}_{x/y}$. Paths $\Gamma_{x,y}$ and $\tilde{\Gamma}_{x,y}$ are shown in Fig. 2(a). $W_{1/2}$ takes the value of ± 1 and can be interpreted as a closed transport of ε -particles across a x/y -oriented

non-contractible loop of the torus (see below). One can also define two t'Hooft operators T_1 and T_2 which commutes with all the $A_v B_{p(v)}$ and B_p but respectively anti-commutes with W_1 and W_2 , which read:

$$T_1 = \prod_{l \in \Gamma_y} Z_l, \quad T_2 = \prod_{l \in \Gamma_x} Z_l. \quad (26)$$

As will become clear later, $T_{1/2}$ plays the role of transporting an e -particle across the y/x -oriented non-contractible loop of the torus.

The intermediate dual (spin) space for a periodic system reads $\mathcal{H}_{e\text{-spin}}^{\text{even} \downarrow} \times \mathcal{H}_{\varepsilon\text{-spin}}^{\text{even} \downarrow} \times \mathcal{H}_W$. Here $\mathcal{H}_{e\text{-spin}}^{\text{even} \downarrow}$ stands for the even- \downarrow subspace of the e spins (same for the $\mathcal{H}_{\varepsilon\text{-spin}}^{\text{even} \downarrow}$) due to the constraint Eq. (24). \mathcal{H}_W is a 4-dimension Hilbert space containing two (auxiliary) spins, which we call Wilson loop spins (WLS) as they corresponds to the two Wilson loop degrees of freedom in the original spin system. When establishing the mapping between $\mathcal{H}_{\text{spin}}$ and $\mathcal{H}_{e\text{-spin}}^{\text{even} \downarrow} \times \mathcal{H}_{\varepsilon\text{-spin}}^{\text{even} \downarrow} \times \mathcal{H}_W$, the eigenbasis of all the $A_v B_{p(v)}$, B_p and $W_{1,2}$ will be mapped to the spin Z eigenbasis of e spins, ε spins and WLS, which gives:

$$A_v B_{p(v)} \leftrightarrow \mathbf{Z}_v^e, \quad B_p \leftrightarrow \mathbf{Z}_p^\varepsilon, \quad W_{1,2} \leftrightarrow Z_{1,2}^W. \quad (27)$$

The t'Hooft operators are mapped to the Pauli X matrices of the WLS: $T_{1,2} \leftrightarrow X_{1,2}^W$. Note that there is an implicit projection operator P in the dual spin operators, which projects states to the even- \downarrow subspace of e and ε spins. Since the physical dual spin subspace states contains only an even number of (e and ε) down spins, a single \mathbf{X}_v^e or \mathbf{X}_p^ε has no matrix element in this subspace because they only mix states with different number of down spins. On the other hand, bilinears of \mathbf{X}_v^e or \mathbf{X}_p^ε have non-zero matrix elements in the physical subspace. For convenience, we take vertex/plaquette 1 as a “reference” vertex/plaquette (see Fig. 2(b)), and looked for the dual operators of $\mathbf{X}_1^e \mathbf{X}_v^e$ and $\mathbf{X}_1^e \mathbf{X}_p^\varepsilon$ such that the algebraic relations in Eq. (14) can be satisfied. One possible choice is the following mapping:

$$\prod_{l \in \Gamma_{1,v}} Z_l \leftrightarrow \mathbf{X}_1^e \mathbf{X}_v^e, \quad (28)$$

$$\prod_{l \in \Gamma_{1,v}} Z_l \prod_{l' \in \tilde{\Gamma}_{1,p}} X_{l'} \leftrightarrow \mathbf{X}_1^e \mathbf{X}_p^\varepsilon \quad (29)$$

Here $\Gamma_{1,v}$ ($\tilde{\Gamma}_{1,p}$) is a direct (dual) lattice path connecting the vertices 1 and v (plaquettes 1 and p), see Fig. 2(b) for a schematic of them. To simplify the notation, we are simply using the sequence numbers of vertices and plaquettes to denote them in the subindices of the operators (see their order in Fig. 2(b)).

The mapping from e spins (ε spins) to the e bosons (ε fermions) is very similar to the infinite lattice case shown in Eqs. (17) and (18), however, due to the constraints in Eq. (24), the (physical) e - and ε -particle states contains only an even number of particles. The dual boson-fermion (and WLS) space reads: $\mathcal{H}_e^{\text{even}} \times \mathcal{H}_\varepsilon^{\text{even}} \times \mathcal{H}_W$.

Note that the sequence of plaquettes in the Jordan-Wigner transformation between ε spins and ε fermions has also changed now (which is shown in Fig. 2(b)). In this way, one obtains the duality mapping between $\mathcal{H}_{\text{spin}}$ and $\mathcal{H}_e^{\text{even}} \times \mathcal{H}_\varepsilon^{\text{even}} \times \mathcal{H}_W$, local X_l and $X_l Z_{\text{SW}(l)}$ operators are mapped to:

I). l is a vertical link

i). $l \notin \Gamma_y$ and l does not cross $\tilde{\Gamma}_x$.

$$Z_l \leftrightarrow (b_{v_1} + b_{v_1}^\dagger)(b_{v_2} + b_{v_2}^\dagger) \left(\prod_{l \times \tilde{\Gamma}_{1,p}} -i\gamma_p \gamma'_p \right), \quad (30a)$$

$$X_l Z_{\text{SW}(l)} \leftrightarrow i\gamma_p \gamma'_p. \quad (30b)$$

ii). $l \in \Gamma_y$ and l does not cross $\tilde{\Gamma}_x$.

$$Z_l \leftrightarrow (b_{v_1} + b_{v_1}^\dagger)(b_{v_2} + b_{v_2}^\dagger), \quad (31a)$$

$$X_l Z_{\text{SW}(l)} \leftrightarrow \left[\prod_{l \in \Gamma_{1,v}} (-1)^{b_v^\dagger b_v} \right] i\gamma_{p_1} \gamma'_{p_2} Z_1^W. \quad (31b)$$

iii). $l \notin \Gamma_y$ and l crosses $\tilde{\Gamma}_x$.

$$Z_l \leftrightarrow (b_{v_1} + b_{v_1}^\dagger)(b_{v_2} + b_{v_2}^\dagger) \left(\prod_{l \times \tilde{\Gamma}_{1,p}} -i\gamma_p \gamma'_p \right) X_1^W, \quad (32a)$$

$$X_l Z_{\text{SW}(l)} \leftrightarrow i\gamma_{p_1} \gamma'_{p_2}. \quad (32b)$$

iv). $l \in \Gamma_y$ and l crosses $\tilde{\Gamma}_x$.

$$Z_l \leftrightarrow (b_{v_1} + b_{v_1}^\dagger)(b_{v_2} + b_{v_2}^\dagger) X_1^W, \quad (33a)$$

$$X_l Z_{\text{SW}(l)} \leftrightarrow i\gamma_p \gamma'_p Z_1^W. \quad (33b)$$

II). l is a horizontal link

i). $l \notin \Gamma_x$ and l does not cross $\tilde{\Gamma}_y$.

$$Z_l \leftrightarrow (b_{v_1} + b_{v_1}^\dagger)(b_{v_2} + b_{v_2}^\dagger), \quad (34a)$$

$$X_l Z_{\text{SW}(l)} \leftrightarrow \left[\prod_{l \in \Gamma_{1,v}} (-1)^{b_v^\dagger b_v} \right] i\gamma_{p_1} \gamma'_{p_2}. \quad (34b)$$

ii). $l \in \Gamma_x$ and l does not cross $\tilde{\Gamma}_y$.

$$Z_l \leftrightarrow (b_{v_1} + b_{v_1}^\dagger)(b_{v_2} + b_{v_2}^\dagger), \quad (35a)$$

$$X_l Z_{\text{SW}(l)} \leftrightarrow \left[\prod_{l \in \Gamma_{1,v}} (-1)^{b_v^\dagger b_v} \right] i\gamma_{p_1} \gamma'_{p_2} Z_2^W. \quad (35b)$$

iii). $l \notin \Gamma_x$ and l crosses $\tilde{\Gamma}_y$.

$$Z_l \leftrightarrow (b_{v_1} + b_{v_1}^\dagger)(b_{v_2} + b_{v_2}^\dagger) \left(\prod_{l \times \tilde{\Gamma}_{1,p}} -i\gamma_p \gamma'_p \right) X_2^W, \quad (36a)$$

$$X_l Z_{\text{SW}(l)} \leftrightarrow i\gamma_{p_1} \gamma'_{p_2}. \quad (36b)$$

iv). $l \in \Gamma_x$ and l crosses $\tilde{\Gamma}_y$.

$$Z_l \leftrightarrow (b_{v_1} + b_{v_1}^\dagger)(b_{v_2} + b_{v_2}^\dagger) X_2^W, \quad (37a)$$

$$X_l \leftrightarrow i\gamma_{p_1} \gamma'_{p_2} Z_2^W. \quad (37b)$$

Here for a horizontal (vertical) link l , v_1 and v_2 are the two vertices connected by it, p_1 and p_2 are the plaquettes to its top (left) and bottom (right). Again, the non-local boson and fermion parities in the dual operators reflect the semionic statistical interaction between e and ε particles. Moreover, when an e (ε) particle is moving across the x/y -direction boundary, there will be an associated $X_{2/1}^W$ ($Z_{1/2}^W$) operator. The spin Z configuration of WLS determines the boundary condition of ε particles.

III. MODEL HAMILTONIAN

In this study, we consider Hamiltonians of the form: $H = H_0 + H_1$. H_0 commutes with $A_v B_{\mathbf{p}(v)}$ for $\forall v$, according to the boson-fermion mapping introduced in Sec. II B, its dual operator has dynamical (ε) fermions and static π -fluxes (e particles). Many exactly solvable models can be constructed from these type of Hamiltonians by making the fermions free, e.g., the Kitaev honeycomb model [10–13]. H_1 will be a term that allows the motion of e particles, while preserving their total number. We choose H_0 to be given by:

$$\begin{aligned}
H_0 = & \sum_{l \in h\text{-link}} -J_x X_l Z_{\text{SW}(l)} + J_y Y_l Y_{\text{SE}(l)} - J_z X_{\text{NE}(l)} Z_l + \kappa [Z_l Z_{\text{SW}(l)} Y_{\text{SE}(l)} + X_l X_{\text{NE}(l)} Y_{\text{SE}(l)} - Y_l Z_{\text{SE}(l)} X_{\text{NE}(l)}] \\
& + \sum_{l \in v\text{-link}} \kappa [Y_l Z_{\text{SW}(l)} X_{\text{NE}(l)} - Z_l Z_{\text{SW}(l)} Y_{\text{NW}(l)} - X_l X_{\text{NE}(l)} Y_{\text{NW}(l)}].
\end{aligned} \tag{38}$$

Here h/v -link stands for horizontal/vertical links. This Hamiltonian is equivalent to the Kitaev honeycomb Hamiltonian (with a Haldane mass term κ) [13] by plaing the sites of the original honeycomb lattice onto the links of a square lattice (see Supplementary Section S-III [20]

for a schematic of the lattice) and a unitary transformation U which transforms:

$$X_j \leftrightarrow Z_j, Y_j \rightarrow -Y_j, \forall j \in A\text{-sublattice}. \tag{39}$$

Under the duality transformation introduced in Sec. II B, the dual Hamiltonian reads (for an infinite system):

$$\begin{aligned}
\tilde{H}_0 = & - \sum_p \left(J_x e^{i\pi\beta_{\mathbb{L}(p,p+\hat{y})}} i\gamma_{p+\hat{y}} \gamma'_p + J_y e^{i\pi\beta_{\mathbb{L}(p,p+\hat{x})}} i\gamma_{p+\hat{x}} \gamma'_p + J_z i\gamma_p \gamma'_{p+\hat{x}} \right) \\
& - \kappa \sum_p \left[e^{i\pi\beta_{\mathbb{L}(p,p+\hat{y})}} i\gamma_{p+\hat{y}} \gamma'_{p-\hat{x}} + e^{i\pi b_{v(p)}^\dagger b_{v(p)}} i\gamma_{p-\hat{x}} \gamma_p + e^{i\pi\beta_{\mathbb{L}(p,p+\hat{y})}} i\gamma_p \gamma_{p+\hat{y}} \right. \\
& \left. + e^{i\pi\beta_{\mathbb{L}(p-\hat{x},p-\hat{x}+\hat{y})}} i\gamma'_{p+\hat{y}} \gamma'_p + i\gamma'_{p+\hat{x}} \gamma'_p + e^{i\pi\beta_{\mathbb{L}(p,p-\hat{y})}} i\gamma'_{p-\hat{y}} \gamma'_{p+\hat{x}} \right].
\end{aligned} \tag{40}$$

Here $\tilde{\mathbb{L}}(p, p')$ stands for the link sandwiched by plaquettes p and p' , $\beta_l = \sum_{v \in L(l)} b_v^\dagger b_v$ for a horizontal link l (here $L(l)$ stands for the vertices to the left of link l). It is clear that \tilde{H}_0 has a Bogoliubov-de Gennes (BdG) form for the ε fermions in a background of static π -fluxes (e particles), and can be solved exactly within any given real-space configuration of e particles.

As for H_1 , we choose it to be:

$$H_1 = g \sum_l Z_l \frac{1 - A_{v_1(l)} B_{\mathbf{p}(v_1(l))} A_{v_2(l)} B_{\mathbf{p}(v_2(l))}}{2}, \tag{41}$$

with $v_1(l)$ and $v_2(l)$ being the two vertices adjacent to link l . Its dual operator \tilde{H}_1 , according to Eqs. (17) and (23), reads (for the infinite lattice case):

$$\begin{aligned}
\tilde{H}_1 = & g \sum_v b_v^\dagger b_{v+\hat{y}} \prod_{p \in R(\mathbb{L}(v, v+\hat{y}))} (-i\gamma_p \gamma'_p) \\
& + b_v^\dagger b_{v+\hat{x}} + h.c.
\end{aligned} \tag{42}$$

$\sim b_{v_1}^\dagger b_{v_2} + b_{v_2}^\dagger b_{v_1}$, Here $\mathbb{L}(v, v')$ stands for the link connecting vertices v and v' , $R(l)$ stands for the plaquettes to the link l . Notice that the above Hamiltonian is a sum of operators that act on spins contained within some local region of the link l , and therefore it is a strictly local perturbation (even though it contains products of several spin operators). So \tilde{H}_1 contains nearest-neighbor e -particle hopping terms. Note that it is also dressed by

ε particles' parities due to the statistical interaction between e and ε particles. To perform calculations, in this study, H_1 will be treated as a perturbation to H_0 .

IV. BERRY PHASES OF VISONS

A. Kitaev model with a Haldane mass term

We will use the previously described mapping to compute the Berry phase for transporting the π -flux in a closed loop around a single plaquette. This phase can be viewed as a universal characterization of the topologically ordered state enriched by lattice translational symmetry [22–28].

In order to compute the Berry phase, we place two e particles far apart on a torus, and will allow only one of them to move within the 4 vertices surrounding a plaquette (see inset Fig. 3(a)). This is accomplished by only adding the flux-hopping operator, from Eq. (41), to be non-zero at the links connecting these 4 vertices. For a fixed WLS configuration $|z_1, z_2\rangle$, when the mobile e -particle is located at site $j \in \{1, 2, 3, 4\}$, the corresponding *physical* (even number of ε particles) ground state of \tilde{H}_0 reads:

$$|\Phi_j\rangle = b_0^\dagger b_j^\dagger |0\rangle \otimes |\Psi_j^\varepsilon\rangle \otimes |z_1, z_2\rangle. \tag{43}$$

Here $|\Psi_j^\varepsilon\rangle$ is the even-parity ground state of a BdG Hamiltonian with two π fluxes at 0 and j , and the $z_{1,2} = \pm 1$

are the eigenvalues of the Wilson loop operators that label the global periodic/antiperiodic boundary conditions of the fermions along the x - and y -directions (see Supplementary Section S-III [20]). $|\Psi_j^\varepsilon\rangle$ can be solved exactly and has a BCS form (see Supplementary [20]). The Berry phase for this close-loop movement of an e -particle is: $e^{i\phi} \approx \prod_{j=1}^4 \langle \Phi_{j+1} | Z_{j+1,j} | \Phi_j \rangle$. Note that the index j runs cyclically from 1 to 4, i.e., $|\Phi_5\rangle \equiv |\Phi_1\rangle$. In the dual space, the Berry phase reads:

$$e^{i\phi} = \langle \Psi_1^\varepsilon | \left(\prod_{p \in L(4,1)} -i\gamma_p \gamma'_p \right) | \Psi_4^\varepsilon \rangle \langle \Psi_4^\varepsilon | \Psi_3^\varepsilon \rangle \times \langle \Psi_3^\varepsilon | \left(\prod_{p \in L(3,2)} -i\gamma_p \gamma'_p \right) | \Psi_2^\varepsilon \rangle \langle \Psi_2^\varepsilon | \Psi_1^\varepsilon \rangle. \quad (44)$$

Here $L(4,1)$ denotes the string of plaquettes to the left of link $(4,1)$ that runs until the left edge of the torus.

In our study, we take the following parameters: $J_x = J_z = 1, \kappa = 0.1$. The torus has $N \times N$ plaquettes with N even. We consider two values $J_y = \pm 1$ which corresponds to fermionic BdG states with Chern numbers $C = \pm 1$. There are 4 high-symmetry points (HSPs) in k -space which are unpaired in a BdG Hamiltonian [12, 29, 30]: $(0,0)$, $(\pi,0)$, $(0,\pi)$ and (π,π) . For $J_y = 1$, the fermion band energy $\epsilon(0,0) < 0$ and is positive at other three HSPs. In this case, we have found that the single-plaquette Berry phase $\phi \rightarrow 0$ with increasing N for any BC. On the other hand, for $J_y = -1$, $\epsilon(\mathbf{k}) < 0$ at $(0,0)$, $(\pi,0)$ and $(0,\pi)$, and is positive at (π,π) . For this case we have found that for any BC, $\phi \rightarrow \pi$ as N increases. The results are presented in Fig. 3(a) and this is one of the main findings of our study.

The motion of the vison in the ferromagnetic (FM) and antiferromagnetic (AFM) Kitaev models induced by physically realistic perturbations such as the Zeemann field, has also been studied in Refs. [31, 32]. While an earlier version of Ref. [31] had concluded that the phase of vison in the FM model was π around a unit cell, the updated understanding provided in Refs. [31, 32] is currently in mutual agreement with the conclusion that the vison acquires zero phase in the FM model and π phase in the AFM model around a unit cell, which is also in agreement with the current study.

We also studied the braiding phases for two anyons. To avoid geometric phases depending on the details of the braiding path, we follow the Levin-Wen protocol [13, 33, 34]. Fig. 3(b) presents results of the braiding phases. For $J_y = 1$, with increasing system size, the braiding phase $\phi \rightarrow -\pi/8$ for anti-periodic BC (APBC) and $\phi \rightarrow 3\pi/8$ for periodic BC (PBC). While for $J_y = -1$, the $\phi \rightarrow \pi/8$ for APBC and $\phi \rightarrow -3\pi/8$ for PBC. Our results for ϕ match exactly the prediction of $R_1^{\sigma,\sigma} \propto \exp(-iC\pi/8)$ and $R_e^{\sigma,\sigma} \propto \exp(iC3\pi/8)$ in Ref. [13] (here σ stands for the π -flux particle). The difference between PBC and APBC originates from the fermion ground state parity of \tilde{H}_0 . The state with $J_y = 1$ is a $p+ip$ topological

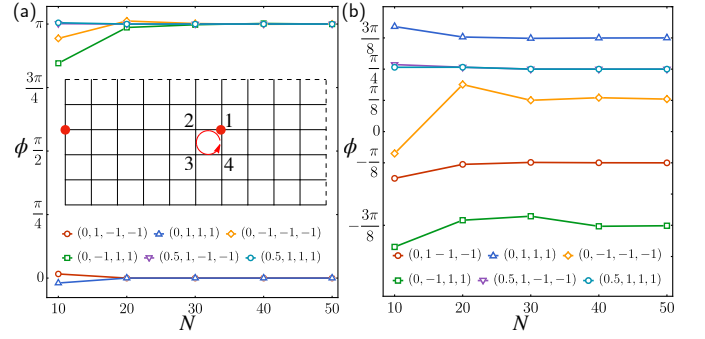


FIG. 3. Berry phase for e particles. (a) Berry phase for a single-plaquette movement of an e -particle. $\phi \rightarrow 0$ or π in the thermodynamic limit. The inset indicates the set-up of numerical calculations: two e particles are highlighted by the red dots with one of them hops circularly between the 4 sites. The legends indicate values of parameters (t, J_y, z_1, z_2) in the model. (b) Berry phase for the exchange of two e particles. ϕ converges to predicted values in Ref.[13] as $N \rightarrow \infty$.

superconductor, and the ground state would have an odd number of fermions under PBC [35], which is unphysical in our case. Since, only even-parity states are physical, the lowest energy physical eigenstate of \tilde{H}_0 in this case is actually the first excited state of the BdG Hamiltonian with a single Bogoliubov quasiparticle. Thus for PBCs the π -fluxes are in the fusion sector $\sigma \times \sigma = \varepsilon$, explaining the difference in braidings that we observe in Fig. 3. As for APBC, the ground state of the BdG Hamiltonian contains an even number of fermions, therefore the π -fluxes are in the fusion sector $\sigma \times \sigma = 1$.

B. Higher Chern numbers and conjecture for arbitrary case

One can also explore cases with higher Chern numbers by correspondingly modifying H_0 . This illustrates the power of this construction allowing to write an exactly solvable model for any free fermion Hamiltonian of interest. We accomplished this explicitly by introducing some 4-spin interaction terms to H_0 in Eq. (38):

$$\begin{aligned} & \frac{t}{2} \left[\sum_{l \in h\text{-link}} (Y_l Z_{SW(l)} Z_{NE(l)} Y_{N(l)} + Y_l Y_{W(l)} X_{SW(l)} X_{NE(l)}) \right. \\ & + \sum_{l \in v\text{-link}} (Y_l Y_{S(l)} X_{SW(l)} X_{NE(l)} + Y_l Y_{E(l)} Z_{SW(l)} Z_{NE(l)}) \\ & \left. + \sum_p B_p + \sum_v A_v \right]. \quad (45) \end{aligned}$$

The $E(l)$ ($S(l)$) stands for the link to the east (south) of l within a common plaquette. Under the duality mapping established in this work, these new terms are mapped to

third-neighbor Majorana fermion couplings of the form:

$$t \sum_p (-i\gamma_p \gamma'_p - i\gamma_p \gamma'_{p+2\hat{x}} - i\gamma_p \gamma'_{p-2\hat{y}}). \quad (46)$$

Here for simplicity we have omitted the non-local vison parities and the WLS operators involved in some of the terms, for the complete expression see Supplementary Section III [20].

At $J_y = 1$, $t = 0.5$, \tilde{H}_0 has $C = -2$. $\epsilon_k < 0$ at all HSPs, so for both PBC and APBC, the fermion ground state parity of \tilde{H}_0 is even. There are two types of anyons in this case [13] and we studied the sector with $a \times \bar{a} = 1$ where a and \bar{a} denote the two kinds of π -flux particles in these states. When braiding a single e -particle around a plaquette, we found Berry phase $\phi = \pi$ for any BC. As for the braiding phase, we obtained $R_1^{a,\bar{a}} = e^{i\pi/4} = e^{-iC\pi/8}$, which is also consistent with Ref. [13]. More details can be found in Supplementary Information [20].

As mentioned before, the phase ϕ acquired by a π -flux upon enclosing a plaquette is a universal characteristic of the symmetry enriched topological state. BdG states of fermions with lattice translations can be classified by their Chern number, $C \in \mathbb{Z}$, and 4 parity indices ζ_k , which dictate whether the band is inverted ($\zeta_k = -1$) or not ($\zeta_k = 1$) in each of the 4 HSPs of the Brillouin zone [12, 29, 30, 36–39]. Therefore the value of ϕ should be a function uniquely fixed by C and ζ_k . The analytical proof of the value of ϕ in the most general case is not known to us. Ref. [12] showed that when $C = 0$, $\phi = 0$ when all $\zeta_k = 1$ and $\phi = \pi$ when all $\zeta_k = -1$ (all HSP are band-inverted), in agreement with previous arguments [23]. Ref. [12] also showed that the cases with $C = 0$ and only two $\zeta_k = -1$, corresponds to states with “weak symmetry breaking” (and thus the π -fluxes cannot be transported to adjacent vertices with local operations). We have shown here that when only one $\zeta_k = -1$ and $C = 1$ then $\phi = 0$, and when three $\zeta_k = -1$ and $C = -1$ then $\phi = \pi$. We also showed that when $C = -2$ and all four $\zeta_k = -1$, then $\phi = \pi$. This suggest the conjecture that for states with odd C and only one $\zeta_k = -1$, then $\phi = 0$ and states with three $\zeta_k = -1$ then $\phi = \pi$. For states with even C and all $\zeta_k = 1$ then $\phi = 0$ and those with all four $\zeta_k = -1$ then $\phi = \pi$ (states with even C and only two $\zeta_k = -1$ should display weak symmetry

breaking of translations [12]).

V. DISCUSSIONS

We have established an *exact* mapping between a 2D spin system and a 2D boson-boson (e, m) or boson-fermion (e, ε) system, where the two types of particles in the dual space are mutual semions, which generalizes the previous dual maps that relied on imposing local \mathbb{Z}_2 constraints [10]. This amounts to constructing explicit vison and spinon non-local creation/annihilation operators in terms of the underlying spin degrees of freedom. Based on this mapping, we found that the Berry phase for the transport of the vison (π -flux excitation) around a single plaquette was quantized to be 0 or π . We have conjectured a universal form of this phase that depends on the Chern number and the parity indices at HSPs of the BdG band structure of the spinons, generalizing previous results from non-chiral states in Refs. [12, 23] to chiral and non-abelian states. We also computed explicitly the braiding phase between two visons, which was found to be consistent with the general arguments of Ref. [13] for both $C = 1$ and $C = 2$ states of the spinons. In the models studied here, the e -particles are static and we only need to solve a free fermionic Hamiltonian of $N^2 \times N^2$. Thus the Berry phase for e -particle movement can be calculated even for relatively large system sizes without too much computational cost. The lattice dualities developed in this work are universal and can be used to study not only the Berry phases of translations of visons but many other topological and dynamical properties of these excitations, such as their effective mass and dispersions, which can be crucial in understanding their role in real materials and experiments [31].

ACKNOWLEDGMENTS

C.C. thanks Guo-Yi Zhu for enlightening discussions. C.C. and P.R. thank Professor Peter Fulde for kind encouragement on pursuing this project. C.C. acknowledges the support from Shuimu Tsinghua Scholar Program.

-
- [1] X.-G. Wen, *Quantum Field Theory of Many-Body Systems* (Oxford University Press, 2010).
 - [2] E. Fradkin, *Field Theories of Condensed Matter Physics*, 2nd ed. (Cambridge University Press, 2013).
 - [3] P. W. Anderson, The resonating valence bond state in La₂CuO₄ and superconductivity, *Science* **235**, 1196 (1987).
 - [4] G. Baskaran, Z. Zou, and P. W. Anderson, The resonating valence bond state and high- T_c superconductivity — a mean field theory, *Solid State Commun.* **63**, 973 (1987).

- [5] N. Read and B. Chakraborty, Statistics of the excitations of the resonating-valence-bond state, *Phys. Rev. B Condens. Matter* **40**, 7133 (1989).
- [6] S. Kivelson, Statistics of holons in the quantum hard-core dimer gas, *Phys. Rev. B Condens. Matter* **39**, 259 (1989).
- [7] N. Read and S. Sachdev, Large- N expansion for frustrated quantum antiferromagnets, *Phys. Rev. Lett.* **66**, 1773 (1991).
- [8] T. Senthil and M. P. A. Fisher, \mathbb{Z}_2 gauge theory of electron fractionalization in strongly correlated systems,

- Phys. Rev. B Condens. Matter* **62**, 7850 (2000).
- [9] A. Y. Kitaev, Fault-tolerant quantum computation by anyons, *Ann. Phys.* **303**, 2 (2003).
 - [10] Y.-A. Chen, A. Kapustin, and Đ. Radičević, Exact bosonization in two spatial dimensions and a new class of lattice gauge theories, *Ann. Phys.* **393**, 234 (2018).
 - [11] O. Pozo, P. Rao, C. Chen, and I. Sodemann, Anatomy of Z_2 fluxes in anyon fermi liquids and bose condensates, *Phys. Rev. B* **103**, 035145 (2021).
 - [12] P. Rao and I. Sodemann, Theory of weak symmetry breaking of translations in Z_2 topologically ordered states and its relation to topological superconductivity from an exact lattice Z_2 charge-flux attachment, *Phys. Rev. Research* **3**, 023120 (2021).
 - [13] A. Kitaev, Anyons in an exactly solved model and beyond, *Ann. Phys.* **321**, 2 (2006).
 - [14] H.-D. Chen and J. Hu, Exact mapping between classical and topological orders in two-dimensional spin systems, *Phys. Rev. B* **76**, 193101 (2007).
 - [15] H.-D. Chen and Z. Nussinov, Exact results of the kitaev model on a hexagonal lattice: spin states, string and brane correlators, and anyonic excitations, *Journal of Physics A: Mathematical and Theoretical* **41**, 075001 (2008).
 - [16] E. Cobanera, G. Ortiz, and Z. Nussinov, Unified approach to quantum and classical dualities, *Phys. Rev. Lett.* **104**, 020402 (2010).
 - [17] E. Cobanera, G. Ortiz, and Z. Nussinov, The bond-algebraic approach to dualities, *Advances in Physics* **60**, 679 (2011).
 - [18] Z. Nussinov, G. Ortiz, and E. Cobanera, Arbitrary dimensional majorana dualities and architectures for topological matter, *Phys. Rev. B* **86**, 085415 (2012).
 - [19] A. Kapustin and L. Fidkowski, Local commuting projector hamiltonians and the quantum hall effect, *Commun. Math. Phys.* **373**, 763 (2020).
 - [20] Additional details are provided in the supplementary information file which includes references 12, 13, 33, 34, 40, and 41.
 - [21] Here the fact that the statistical interaction only appears when e and m particles are pair fluctuating or hopping along the y -direction can be understood as due to the specific “gauge choice” in our duality mapping: each e (m) particle produces a “branch-cut” in the vector potential to the right (left) infinity, which is felt by the m (e) particles.
 - [22] X.-G. Wen, Quantum orders and symmetric spin liquids, *Phys. Rev. B* **65**, 165113 (2002).
 - [23] A. M. Essin and M. Hermele, Classifying fractionalization: Symmetry classification of gapped F_2 spin liquids in two dimensions, *Phys. Rev. B* **87**, 104406 (2013).
 - [24] M. Barkeshli, P. Bonderson, M. Cheng, and Z. Wang, Symmetry fractionalization, defects, and gauging of topological phases, *Phys. Rev. B* **100**, 115147 (2019).
 - [25] Y.-M. Lu and A. Vishwanath, Classification and properties of symmetry-enriched topological phases: Chernsimons approach with applications to Z_2 spin liquids, *Phys. Rev. B* **93**, 155121 (2016).
 - [26] X.-G. Wen, Quantum orders in an exact soluble model, *Phys. Rev. Lett.* **90**, 016803 (2003).
 - [27] S.-P. Kou, M. Levin, and X.-G. Wen, Mutual chernsimons theory for Z_2 topological order, *Phys. Rev. B* **78**, 155134 (2008).
 - [28] A. Mesaros and Y. Ran, Classification of symmetry enriched topological phases with exactly solvable models, *Phys. Rev. B* **87**, 155115 (2013).
 - [29] S.-P. Kou and X.-G. Wen, Translation-symmetry-protected topological orders in quantum spin systems, *Phys. Rev. B* **80**, 224406 (2009).
 - [30] S.-P. Kou and X.-G. Wen, Translation-invariant topological superconductors on a lattice, *Phys. Rev. B* **82**, 144501 (2010).
 - [31] A. P. Joy and A. Rosch, Dynamics of visons and thermal Hall effect in perturbed Kitaev models, arXiv e-prints (2021), [arXiv:2109.00250 \[cond-mat.str-el\]](#).
 - [32] C. Chen and I. Sodemann Villadiego, The nature of visons in the perturbed ferromagnetic and antiferromagnetic Kitaev honeycomb models, arXiv e-prints (2022), [arXiv:2207.09492 \[cond-mat.str-el\]](#).
 - [33] M. Levin and X.-G. Wen, Fermions, strings, and gauge fields in lattice spin models, *Phys. Rev. B* **67**, 245316 (2003).
 - [34] K. Kawagoe and M. Levin, Microscopic definitions of anyon data, *Phys. Rev. B* **101**, 115113 (2020).
 - [35] N. Read and D. Green, Paired states of fermions in two dimensions with breaking of parity and time-reversal symmetries and the fractional quantum hall effect, *Phys. Rev. B* **61**, 10267 (2000).
 - [36] M. Sato, Topological odd-parity superconductors, *Phys. Rev. B* **81**, 220504 (2010).
 - [37] M. Sato and S. Fujimoto, Existence of majorana fermions and topological order in nodal superconductors with spin-orbit interactions in external magnetic fields, *Phys. Rev. Lett.* **105**, 217001 (2010).
 - [38] M. Geier, P. W. Brouwer, and L. Trifunovic, Symmetry-based indicators for topological bogoliubov-de gennes hamiltonians, *Phys. Rev. B* **101**, 245128 (2020).
 - [39] S. Ono, H. C. Po, and H. Watanabe, Refined symmetry indicators for topological superconductors in all space groups, *Science Advances* **6**, eaaz8367 (2020).
 - [40] M. Cheng, R. M. Lutchyn, V. Galitski, and S. Das Sarma, Tunneling of anyonic majorana excitations in topological superconductors, *Phys. Rev. B* **82**, 094504 (2010).
 - [41] L. M. Robledo, Sign of the overlap of hartree-fock-bogoliubov wave functions, *Phys. Rev. C* **79**, 021302 (2009).

Berry Phases of Vison Transport in \mathbb{Z}_2 Topologically Ordered States from Exact Fermion-Flux Lattice Dualities

Chuan Chen,^{1,2} Peng Rao,² and Inti Sodemann^{3,2}

¹*Institute for Advanced Study, Tsinghua University, 100084 Beijing, China*

²*Max-Planck Institute for the Physics of Complex Systems, 01187 Dresden, Germany*

³*Institut für Theoretische Physik, Universität Leipzig, 04103 Leipzig, Germany*

(Dated: October 10, 2022)

CONTENTS

S-I. Mapping between spin and boson-boson systems	2
S-I.A. Open lattice	2
S-I.B. Periodic lattice	2
S-II. Mapping between spin and boson-fermion systems	4
S-II.A. Open lattice	4
S-II.B. Periodic lattice: examples	5
S-III. Mapping of the Kitaev honeycomb model	6
S-III.A. Kitaev honeycomb model	6
S-III.B. Kitaev model with the Haldane term	7
S-III.C. Generalization to a $C = -2$ model	8
S-IV. Properties of anyons in Kitaev model	9
S-IV.A. Ground state degeneracy of the Kitaev model	9
S-IV.B. Deconfinement of e particles and fluctuation of fermionic ground state parity	10
S-IV.C. Berry phase for a single e particle around a plaquette	10
S-IV.D. Braiding of two e particles	11
S-V. BCS Ansatz without translation invariance	12
S-V.A. The first excited state of a BdG Hamiltonian having an odd ground state parity	14
S-VI. Overlap between BCS states	15
Supplementary References	16

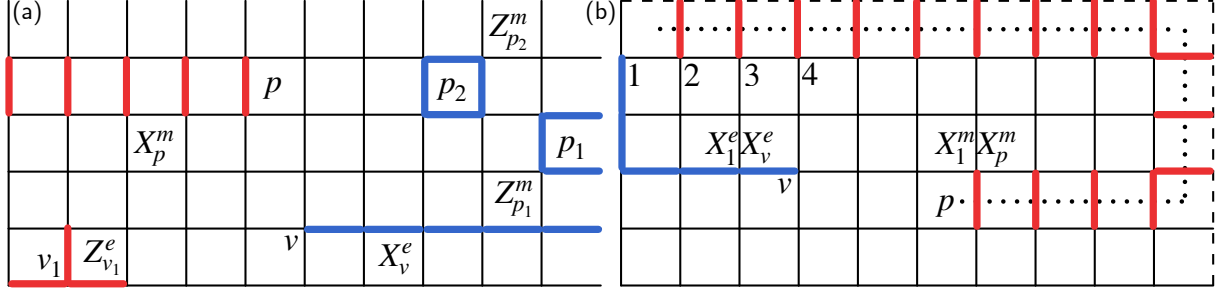


FIG. S1. Representation of operators in open and periodic lattice for the boson-boson mapping. The spin X operators are represented by red links and Z operators are represented by blue links. (a) Operators for an open lattice. The product of X_l operators in \mathbf{X}_p^m terminates at the left end, and the product of Z_l operators in \mathbf{Z}_v^e terminates at the right end. Note at the boundary, there are fewer spin operators involved in the definition of Z_p^m and X_v^e , e.g., see the $Z_{p_1}^m$ and $X_{v_1}^e$ in the figure. (b) Operators for a periodic lattice. The black dots stands for the path $\tilde{\Gamma}_{1,p}$, the path $\Gamma_{1,v}$ is covered by the blue bonds.

S-I. MAPPING BETWEEN SPIN AND BOSON-BOSON SYSTEMS

S-I.A. Open lattice

For a spin system on an open lattice (see Fig. S1(a)), the definition of A_v and B_p are the same as those in the infinite lattice. Note that on an open lattice, there are fewer links involved in the star or plaquette operators at the boundary. For example, at the left or bottom edges there are only 3 links connecting a vertex (2 for the vertex at the left bottom corner); at the right or top edges, there are only 3 links around a plaquette (2 for the one at the top right corner). Therefore, the A_v and B_p operators (which are dual to Z_v^e and Z_p^m respectively) at the edge of the lattice are slightly different from those in the bulk. As for the dual operators of X_v^e and X_p^m , their definitions are similar to those in an infinite lattice, the only difference is that on a finite open lattice, the product of Z_l (X_l) in the dual operator of X_v^e (X_p^m) should terminate at the right (left) boundary. Examples of these operators are shown in Fig. S1. The mappings of local spin Z and X operators are to e and m particles' operators are the same as those in an infinite lattice, which have been presented in the main text.

S-I.B. Periodic lattice

For the case of a periodic lattice, there are now two global constraints:

$$\prod_v A_v = 1, \quad \prod_p B_p = 1. \quad (\text{S1})$$

Therefore, only $N - 1$ A_v (same for B_p) operators are independent with N being the number of unit cells in the lattice, i.e., there are 2^{2N-2} possible configurations of A_v and B_p . To fully label the states in the spin Hilbert space, one needs to introduce two Wilson loop degrees of freedom, the global Wilson loop operators reads:

$$W_1 = \prod_{l \times \tilde{\Gamma}_x} X_l, \quad W_2 = \prod_{l \times \tilde{\Gamma}_y} X_l. \quad (\text{S2})$$

Here $\tilde{\Gamma}_{x/y}$ is a path in the dual lattice (see Fig. 3 in the main text) and the product is taken over the links l which intersect with $\tilde{\Gamma}_{x/y}$, as denoted by the symbol “ \times ”. They can be interpreted as performing the transport of an m -particle around the x/y -oriented non-contractible loops of the torus. On the other hand, the t'Hooft operators are defined as:

$$T_1 = \prod_{l \in \Gamma_y} Z_l, \quad T_2 = \prod_{l \in \Gamma_x} Z_l. \quad (\text{S3})$$

$T_{1,2}$ can be viewed as moving an e -particle along the y, x -oriented non-contractible loops of the torus.

The dual e - and m -spin space consists of even- \downarrow e and m spins, and there is an additional 4-dimensional Hilbert space containing two Wilson loop spins (WLS). The dual Hilbert space reads:

$$\mathcal{H} = \mathcal{H}_e^{\text{even-}\downarrow} \otimes \mathcal{H}_m^{\text{even-}\downarrow} \otimes \mathcal{H}_W. \quad (\text{S4})$$

Since the dual spin space contains an even number of down e and m spins, only bilinear spin X operators have non-zero matrix elements in this physical subspace. For convenience, here we gave chosen vertex (plaquette) 1 as a reference vertex (plaquette), we found that the dual of $X_1^e X_v^e$ and $X_1^m X_p^m$ can be taken as the following form:

$$\prod_{l \in \Gamma_{1,v}} Z_l \leftrightarrow X_1^e X_v^e, \quad \prod_{l \times \tilde{\Gamma}_{1,p}} X_l \leftrightarrow X_1^m X_p^m. \quad (\text{S5})$$

The path $\Gamma_{1,v}$ consists of links of the lattice, which starts from vertex 1, goes down first, then goes to the east until reaching vertex v . The path $\tilde{\Gamma}_{1,p}$ is a dual lattice path, which starts from plaquette 1, goes east first till the end, then goes downawrds, and finally goes west until plaquette p . Example of them are shown in Fig. S1(b). The path $\Gamma_{1,v}$ ($\tilde{\Gamma}_{1,p}$) can be viewed as a *branch-cut* of the e (m) particle at vertex v (plaquette p). The Wilson loop operators are mapped as:

$$W_{1,2} \leftrightarrow Z_{1,2}^W, \quad T_{1,2} \leftrightarrow X_{1,2}^W. \quad (\text{S6})$$

Finally, we shall map $\mathcal{H}_e^{\text{even-}\downarrow} \otimes \mathcal{H}_m^{\text{even-}\downarrow} \otimes \mathcal{H}_W$ to $\mathcal{H}_e^{\text{even}} \times \mathcal{H}_m^{\text{even}} \otimes \mathcal{H}_W$. There are:

$$Z_v^e \leftrightarrow (-1)^{b_v^\dagger b_v}, \quad X_1^e X_v^e \leftrightarrow (b_1 + b_1^\dagger)(b_v + b_v^\dagger), \quad (\text{S7})$$

$$Z_p^m \leftrightarrow (-1)^{d_p^\dagger d_p}, \quad X_1^m X_p^m \leftrightarrow (d_1 + d_1^\dagger)(d_p + d_p^\dagger). \quad (\text{S8})$$

Based on this mapping, one can obtain the mapping of all the local spin X and Z operators. Before presenting the mapping rule, let's first clarify the notation that we will use below, we will study an arbitrary link l aligned vertically (horizontally), the two vertices at the top and bottom (left and right) ends of it are denoted as v_1 and v_2 , the two plaquettes at the left and right (top and bottom) of it are denoted as p_1 and p_2 . The mapping rules of spin X_l and Z_l operators are the following:

I). l is a vertical link

i). l belongs to the bulk, i.e., $l \notin \Gamma_y$ and l does not cross $\tilde{\Gamma}_x$.

$$X_l \leftrightarrow (d_{p_1} + d_{p_1}^\dagger)(d_{p_2} + d_{p_2}^\dagger), \quad (\text{S9a})$$

$$Z_l \leftrightarrow (b_{v_1} + b_{v_1}^\dagger)(b_{v_2} + b_{v_2}^\dagger) \prod_{l \times \tilde{\Gamma}_{1,p}} (-1)^{d_p^\dagger d_p}. \quad (\text{S9b})$$

ii). $l \in \Gamma_y$ and l does not cross $\tilde{\Gamma}_x$.

$$X_l \leftrightarrow \prod_{l \in \Gamma_{1,v}} (-1)^{b_v^\dagger b_v} (d_{p_1} + d_{p_1}^\dagger)(d_{p_2} + d_{p_2}^\dagger) Z_1^W, \quad (\text{S10a})$$

$$Z_l \leftrightarrow (b_{v_1} + b_{v_1}^\dagger)(b_{v_2} + b_{v_2}^\dagger). \quad (\text{S10b})$$

iii). $l \notin \Gamma_y$ and l crosses $\tilde{\Gamma}_x$.

$$X_l \leftrightarrow (d_{p_1} + d_{p_1}^\dagger)(d_{p_2} + d_{p_2}^\dagger), \quad (\text{S11a})$$

$$Z_l \leftrightarrow (b_{v_1} + b_{v_1}^\dagger)(b_{v_2} + b_{v_2}^\dagger) \prod_{l \times \tilde{\Gamma}_{1,p}} (-1)^{d_p^\dagger d_p} X_1^W. \quad (\text{S11b})$$

iv). $l \in \Gamma_y$ and l crosses $\tilde{\Gamma}_x$.

$$X_l \leftrightarrow (d_{p_1} + d_{p_1}^\dagger)(d_{p_2} + d_{p_2}^\dagger) Z_1^W, \quad (\text{S12a})$$

$$Z_l \leftrightarrow (b_{v_1} + b_{v_1}^\dagger)(b_{v_2} + b_{v_2}^\dagger) X_1^W. \quad (\text{S12b})$$

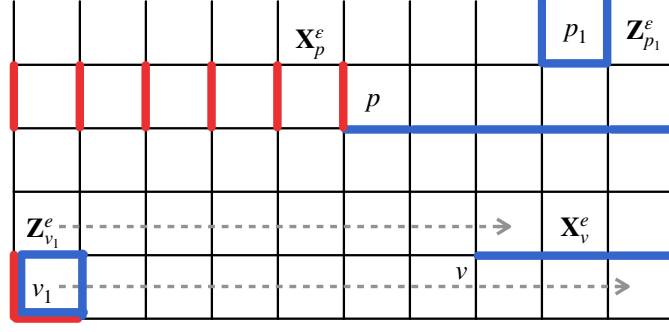


FIG. S2. Operators for the boson-fermion mapping in an open lattice. The gray arrow indicates the sequence of the plaquettes in the Jordan-Wigner transformation from ε spins to ε fermions.

II). l is a horizontal link

i). $l \notin \Gamma_x$ and l does not cross $\tilde{\Gamma}_y$.

$$X_l \leftrightarrow \prod_{l \in \Gamma_{1,v}^e} (-1)^{b_v^\dagger b_v} (d_{p_1} + d_{p_1}^\dagger)(d_{p_2} + d_{p_2}^\dagger), \quad (\text{S13a})$$

$$Z_l \leftrightarrow (b_{v_1} + b_{v_1}^\dagger)(b_{v_2} + b_{v_2}^\dagger). \quad (\text{S13b})$$

ii). $l \in \Gamma_x$ and l does not cross $\tilde{\Gamma}_y$.

$$X_l \leftrightarrow \prod_{l \in \Gamma_{1,v}} (-1)^{b_v^\dagger b_v} (d_{p_1} + d_{p_1}^\dagger)(d_{p_2} + d_{p_2}^\dagger) Z_2^W, \quad (\text{S14a})$$

$$Z_l \leftrightarrow (b_{v_1} + b_{v_1}^\dagger)(b_{v_2} + b_{v_2}^\dagger). \quad (\text{S14b})$$

iii). $l \notin \Gamma_x$ and l crosses $\tilde{\Gamma}_y$.

$$X_l \leftrightarrow (d_{p_1} + d_{p_1}^\dagger)(d_{p_2} + d_{p_2}^\dagger), \quad (\text{S15a})$$

$$Z_l \leftrightarrow (b_{v_1} + b_{v_1}^\dagger)(b_{v_2} + b_{v_2}^\dagger) \prod_{l \times \tilde{\Gamma}_{1,p}} (-1)^{d_p^\dagger d_p} X_2^W. \quad (\text{S15b})$$

iv). $l \in \Gamma_x$ and l crosses $\tilde{\Gamma}_y$.

$$X_l \leftrightarrow (d_{p_1} + d_{p_1}^\dagger)(d_{p_2} + d_{p_2}^\dagger) Z_2^W, \quad (\text{S16a})$$

$$Z_l \leftrightarrow (b_{v_1} + b_{v_1}^\dagger)(b_{v_2} + b_{v_2}^\dagger) X_2^W. \quad (\text{S16b})$$

For $l \in \Gamma_{x/y}$, the dual operator of X_l moves or pair-creates/annihilates the m -particles cross the boundary, it also involves the $Z_{2/1}^W$. Therefore, the value of $Z_{1,2}^W$ controls the boundary conditions of the m -particles. On the other hand, for Z_l with $l \times \tilde{\Gamma}_{x/y}$, its dual not only moves the e -particles cross the boundary, but also involves $X_{1/2}^W$. So e -particle motion cross the boundary will produce dynamical fluctuations of the boundary condition of m -particles.

S-II. MAPPING BETWEEN SPIN AND BOSON-FERMION SYSTEMS

S-II.A. Open lattice

The boson-fermion mapping on an open lattice is the same as the one for an infinite lattice discussed in Section II B of the main text. We choose the plaquette sequence for ε to start from the one at the left bottom, goes to the right within each row and then goes back to the left in the next higher row, as indicated by the gray arrows in Fig. S2. Note that here the A_v and B_p involves fewer links at the boundary. Therefore the product of Z_l in the dual of \mathbf{X}_v^e terminates at the right end of the lattice, and the product of X_l in the dual of \mathbf{X}_p^e terminates at the left boundary of the lattice. See Fig. S2 for a schematic of the operators.

vii).

$$\begin{aligned}
X_{13,14}Z_{1,13} &\leftrightarrow -Z_2^W \left(\prod_{j=14}^{16} \mathbf{z}_j^e \right) \left(\prod_{l=14}^{16} \mathbf{z}_l^\varepsilon \right) \mathbf{x}_1^\varepsilon \mathbf{x}_{13}^\varepsilon \\
&\leftrightarrow (-1)^{\sum_{j=14}^{16} n_j^\varepsilon} i\gamma_{13}\gamma_1' Z_2^W
\end{aligned} \tag{S23}$$

As we can see, operators that transport the ε -particles across the boundary involve $Z_{1,2}^W$, so for a state with a specific value of WLS, e.g., $|\Psi_e\rangle \otimes |\Psi_\varepsilon\rangle \otimes |z_1, z_2\rangle$, the boundary condition of ε particles is determined by $z_{1,2}$. On the other hand, operators that transport the e particles across the boundary contain $X_{1,2}^W$, and will flip the value of $z_{1,2}$ accordingly.

S-III. MAPPING OF THE KITAEV HONEYCOMB MODEL

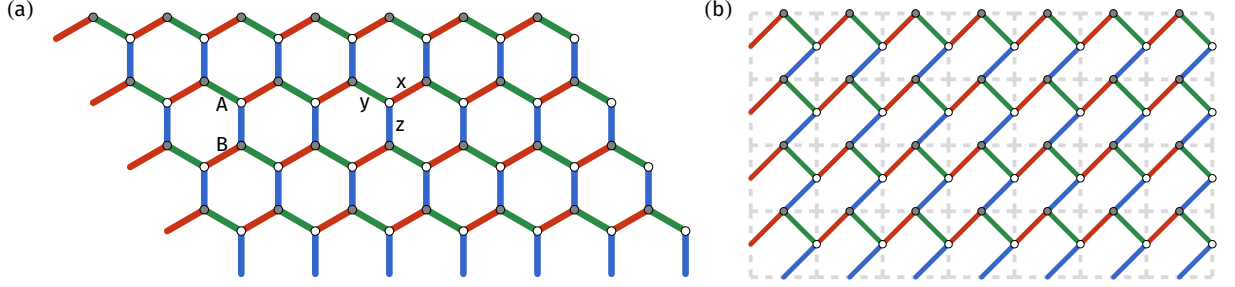


FIG. S4. Schematic of the system. (a) The honeycomb lattice in Kitaev's mode. The x -, y - and z -bond are highlighted by three different colours. (b) The distorted lattice where spins are now located at the edges of a square lattice (gray dashed lines).

S-III.A. Kitaev honeycomb model

In the Kitaev honeycomb model, spins are located at the vertices of a honeycomb lattice, nearest-neighbouring spins are coupled in a Ising-type and the couplings have a directional dependence. The Hamiltonian reads:

$$H_K = -J_x \sum_{x\text{-links}} X_i X_j - J_y \sum_{y\text{-links}} Y_i Y_j - J_z \sum_{z\text{-links}} Z_i Z_j. \tag{S24}$$

Fig. S4(a) is a schematic of the system. The x , y and z bonds are highlighted in red, green and blue colours respectively. In our study, we will do a unitary transformation on the original Kitaev model. The transformation will only affect

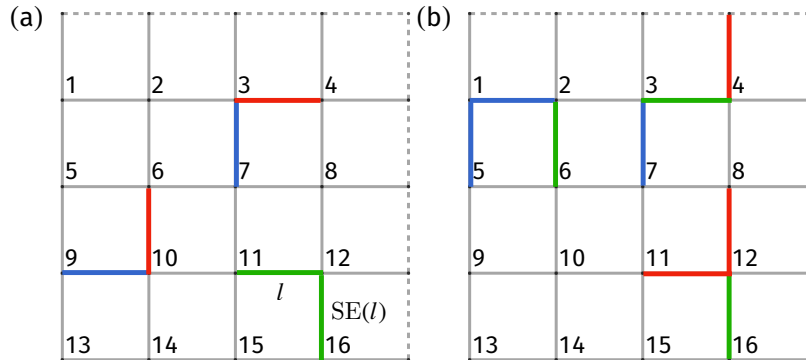


FIG. S5. Example of the couplings in the (transformed) Kitaev Hamiltonian. The green bonds represent spin Y operators.

the spin operators at the A sublattice (indicated by the white disks in Fig. S4):

$$X_j \rightarrow Z_j, \quad Y_j \rightarrow -Y_j, \quad Z_j \rightarrow X_j. \quad (\text{S25})$$

After the transformation, the Hamiltonian changes to:

$$H_K = -J_x \sum_{x\text{-links}} Z_i X_j + J_y \sum_{y\text{-links}} Y_i Y_j - J_z \sum_{z\text{-links}} X_i Z_j. \quad (\text{S26})$$

Here index i in the summation stands for vertices of A sublattice. From now on, we will use H_K to stand for the unitary transformed Kitaev model, unless explicitly mentioned.

The sites of the honeycomb lattice can be identified with links of a square lattice (see Fig. S4(b)). We then denote the local spin operators according to the link they sit. Viewing in terms of a square lattice, the modified Kitaev model now reads:

$$H_K = -J_x \sum_{l \in \text{h-links}} X_l Z_{\text{SW}(l)} + J_y \sum_{l \in \text{h-links}} Y_l Y_{\text{SE}(l)} - J_z \sum_{l \in \text{v-links}} X_l Z_{\text{SW}(l)}. \quad (\text{S27})$$

Here h/v-links stands for the horizontal/vertical links. $\text{SE}(l)$ stands for the link connected with l and located at the southeast of l . A schematic of these operators are shown in Fig. S5(a). Note that a YY coupling can actually be recast into a product of $X_l Z_{\text{SW}(l)}$ and Z_p^ε terms. For instance, in Fig. S5(a), the $Y_{11,12} Y_{16,12}$ can be rewritten as:

$$\begin{aligned} Y_{11,12} Y_{16,12} &= X_{11,12} Z_{11,12} Z_{16,12} X_{16,12} \\ &= X_{11,12} Z_{15,11} Z_{15,11} Z_{11,12} Z_{16,12} Z_{15,16} \\ &\quad Z_{15,16} X_{16,12} \\ &= X_{11,12} Z_{15,11} B_{15} X_{16,12} Z_{15,16}. \end{aligned} \quad (\text{S28})$$

In the main text, the dual Hamiltonian for the infinite lattice case has been given, here we provide the dual Hamiltonian \tilde{H}_K on a periodic system:

$$\begin{aligned} \tilde{H}_K &= -J_x \sum_j \prod_v (-1)^{n_v^e f_{(p,p-\hat{y})}^{\Gamma_{1,v}}} i\gamma_p \gamma'_{p-\hat{y}} (Z_2^W)^{f_{(p,p-\hat{y})}^{\Gamma_x}} \\ &\quad - J_y \sum_p \prod_v (-1)^{n_v^e [f_{(p,p-\hat{y})}^{\Gamma_{1,v}} + f_{(p-\hat{y},p-\hat{y}+\hat{x})}^{\Gamma_{1,v}}]} i\gamma_p \gamma'_{p+\hat{x}-\hat{y}} (Z_1^W)^{f_{(p-\hat{y},p-\hat{y}+\hat{x})}^{\Gamma_y}} (Z_2^W)^{f_{(p,p-\hat{y})}^{\Gamma_x}} \\ &\quad - J_z \sum_p \prod_v (-1)^{n_v^e f_{(p,p+\hat{x})}^{\Gamma_{1,v}}} i\gamma_p \gamma'_{p+\hat{x}} (Z_1^W)^{f_{(p,p+\hat{x})}^{\Gamma_y}}. \end{aligned} \quad (\text{S29})$$

Here the function f_a^b is a conditional function: if a crosses b , it is equal to 1, otherwise it is 0. Note that, e.g., $(p, p+\hat{x})$ is a link in the dual lattice. It is clear that e and ε particles have an statistical interaction and each e particle plays the role of a π flux for the ε particles (and vice versa). It can be seen that the e particle's number at each vertex and the $Z_{1,2}^W$ are good quantum numbers of \tilde{H}_K . So one can diagonalize \tilde{H}_K in a sector with a specific real-space e -particle configuration and a specific configuration of $Z_{1,2}^W$. An eigenstate of \tilde{H}_K is then a product state: $|\Psi\rangle = |n_1^e, \dots\rangle \otimes |\Psi_\varepsilon\rangle \otimes |z_1, z_2\rangle$:

$$\begin{aligned} &\tilde{H}_K |n_1^e, \dots\rangle \otimes |\Psi_\varepsilon\rangle \otimes |z_1, z_2\rangle \\ &= |n_1^e, \dots\rangle \otimes H_\varepsilon(\{n_1^e, \dots\}, z_1, z_2) |\Psi_\varepsilon\rangle \otimes |z_1, z_2\rangle \\ &= E |n_1^e, \dots\rangle \otimes |\Psi_\varepsilon\rangle \otimes |z_1, z_2\rangle. \end{aligned} \quad (\text{S30})$$

So the problem reduces to that of solving the eigenstates of a fermionic BdG Hamiltonian $H_\varepsilon(\{n_1^e, \dots\}, z_1, z_2)$. For a general real-space configuration of e particles, $H_\varepsilon(\{n_1^e, \dots\}, z_1, z_2)$ would not obey translational symmetry. The lowest energy eigenstate of \tilde{H}_K belongs to the sector without any e particle, in that case, $H_\varepsilon(\{n_j^e = 0\}, z_1, z_2)$ describes a translational symmetric p -wave superconductor and (z_1, z_2) determines the boundary condition.

S-III.B. Kitaev model with the Haldane term

In the presence of an external magnetic field, it has been shown that the low energy effective Hamiltonian will include some 3-spin couplings [1]:

$$H_{\text{eff}}^{(3)} = -\kappa \sum_{j,k,l} X_j Y_k Z_l. \quad (\text{S31})$$

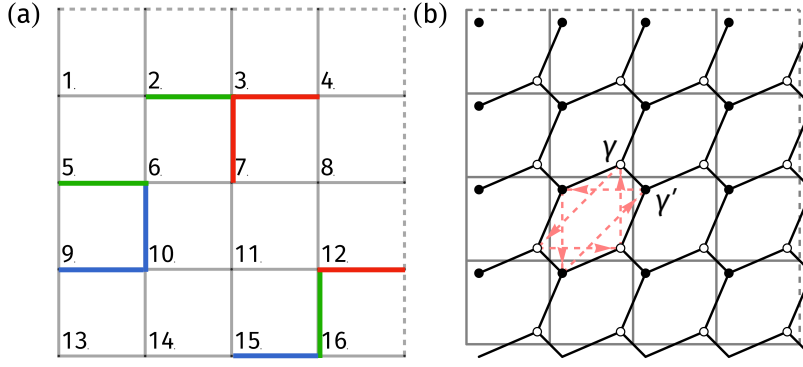


FIG. S6. (a) Some of the Haldane terms involving spins at 2 B-sublattice vertices and 1 A-sublattice vertex. (b) A schematic of the Majorana couplings in the dual Hamiltonian, the local Majorana modes are represented by empty (γ) and filled (γ') disks. The nearest-neighbour couplings are represented by the black bonds, which forms a honeycomb lattice; the Haldane terms are represented by the red coloured arrows (here we are only showing the hoppings within a single hexagon). It is interesting to notice that the couplings between the Majorana modes from our construction has the same type of spatial structure as the one in Kitaev's Majorana representation of the spin operators.

Taking into account the terms where three spins belong to a common hexagon, there will be a Haldane mass term when one write everything in terms of the Majorana fermions. The sum of these operators is denoted as H_H (remember that here we are interested in the unitary transformed operator). We can obtain its dual operator in the BFS space. Fig. S5(b) and Fig. S6(a) show some terms in H_H , and the dual operators of them read:

$$\kappa Z_{5,1} Z_{1,2} Y_{6,2} \leftrightarrow \kappa i \gamma'_5 \gamma'_6, \quad (\text{S32a})$$

$$-\kappa X_{4,16} Y_{3,4} Z_{7,3} \leftrightarrow \kappa (-1)^{n_4^e} i \gamma'_4 \gamma'_7, \quad (\text{S32b})$$

$$\kappa X_{11,12} X_{12,8} Y_{16,12} \leftrightarrow \kappa (-1)^{n_{12}^e} i \gamma'_{16} \gamma'_{12}, \quad (\text{S32c})$$

$$\kappa X_{12,9} Y_{16,12} Z_{15,16} \leftrightarrow \kappa i \gamma_{15} \gamma_{12}, \quad (\text{S32d})$$

$$-\kappa Y_{5,6} Z_{10,6} Z_{9,10} \leftrightarrow \kappa (-1)^{\sum_{j=6}^8 n_j^e} i \gamma_5 \gamma_9, \quad (\text{S32e})$$

$$-\kappa X_{3,4} X_{7,3} Y_{2,3} \leftrightarrow \kappa (-1)^{n_3^e} i \gamma_3 \gamma_2. \quad (\text{S32f})$$

Once obtaining the mapping $H_H \leftrightarrow \tilde{H}_H$, we can then learn the property of $H_K + H_H$ by exploring $\tilde{H} \equiv \tilde{H}_K + \tilde{H}_H$.

The dual Hamiltonian contains Majorana bilinears (in some cases the parity of the e particle and the $Z_{1,2}$ will be involved). We can illustrate the two Majorana modes attached to each plaquette with an empty (γ) and a filled (γ') disk, by connecting the modes that are coupled \tilde{H} , one can see that the Majorana fermions are essentially coupled in the a way as if they are on a honeycomb lattice (see Fig. S6(b)). The original terms in the Kitaev model gives rise to the nearest neighbour hopping (black bonds in Fig. S6(b)), while the Haldane term leads to the next-nearest-neighbour coupling (the couplings within a hexagon are highlighted by the red dashed arrows, the arrow from vertex j to l corresponds to a coupling of the form $i \gamma_l \gamma_j$ or $i \gamma'_l \gamma'_j$).

S-III.C. Generalization to a $C = -2$ model

It is known that the Kitaev model with Haldane term can lead to a Chern number $C = 1$ [1]. In this section, we present a way to generate a model with $C = -2$ by introducing more terms to the model. On the honeycomb lattice, one can add some 4-spin coupling terms. Within each hexagon (see Fig. S7(a)), we add the following terms:

$$X_1 Z_2 X_3 Z_4, Y_2 X_3 Y_4 X_5, Z_3 Y_4 Z_5 Y_6, X_4 Z_5 X_6 Z_1, Y_5 X_6 Y_1 X_2, Z_6 Y_1 Z_2 Y_3. \quad (\text{S33})$$

We choose an overall coupling constant to be $t/2$. In terms of the Majorana representation defined in Kitaev's original paper, these terms corresponds to third neighbor hoppings of the c Majoranas [1]. Under certain parameter regime, the model can give rise to Chern number $C = -2$.

Recall that we need to do a unitary transformation on the spins in even sublattice and distort the lattice into a square lattice. Examples of how each of these terms are mapped are presented below (see Fig. S7(b) and (c) for a

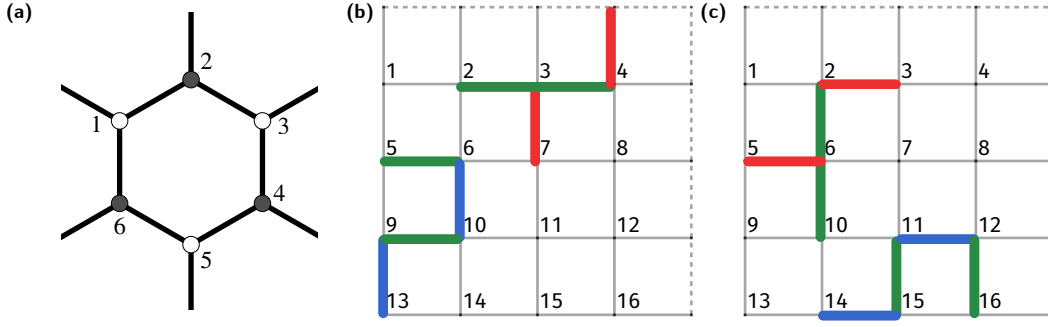


FIG. S7. (a) A schematic of an hexagon. (b) and (c) A schematic of some operators in the t -term.

schematic of some operators):

$$Z_{6,2}Z_{2,3}Z_{7,3}Z_{6,7} \leftrightarrow -i\gamma_6\gamma'_6, \quad (\text{S34a})$$

$$Y_{6,7}Z_{11,7}Y_{10,11}Z_{14,10} \leftrightarrow (-1)^{n_7^e+n_8^e+n_{11}^e+n_{12}^e}(-i\gamma_6\gamma'_{14}), \quad (\text{S34b})$$

$$X_{7,3}Y_{6,7}X_{10,6}Y_{5,6} \leftrightarrow (-1)^{n_6^e}(-i\gamma_5\gamma'_7), \quad (\text{S34c})$$

$$X_{6,7}X_{10,6}X_{5,6}X_{6,2} \leftrightarrow (-1)^{n_6^e}(-i\gamma_6\gamma'_6), \quad (\text{S34d})$$

$$Y_{10,6}X_{5,6}Y_{6,2}X_{2,3} \leftrightarrow (-1)^{n_3^e+n_4^e+n_6^e+n_7^e+n_8^e}(-i\gamma_2\gamma'_{10}), \quad (\text{S34e})$$

$$Z_{5,6}Y_{6,2}Z_{2,3}Y_{7,3} \leftrightarrow -i\gamma_5\gamma'_7. \quad (\text{S34f})$$

The t terms will be mapped to:

$$\begin{aligned} \tilde{H}_t = & \frac{t}{2} \sum_p (1 + (-1)^{n_{\text{SW}(p)}})(-i\gamma_p\gamma'_p) \\ & + (1 + (-1)^{n_{\text{SW}(p+\hat{x})}}) \prod_v (-1)^{n_v^e [f_{(p,p+\hat{x})}^{\Gamma_{1,v}} + f_{(p+\hat{x},p+2\hat{x})}^{\Gamma_{1,v}}]} (-i\gamma_p\gamma'_{p+2\hat{x}}) Z_1^{f_{(p,p+\hat{x})}^{\Gamma_y} + f_{(p+\hat{x},p+2\hat{x})}^{\Gamma_y}} \\ & + (1 + (-1)^{n_{\text{SW}(p-\hat{y})}}) \prod_v (-1)^{n_v^e [f_{(p,p-\hat{y})}^{\Gamma_{1,v}} + f_{(p-\hat{y},p-2\hat{y})}^{\Gamma_{1,v}}]} (-i\gamma_p\gamma'_{p-2\hat{y}}) Z_2^{f_{(p,p-\hat{y})}^{\Gamma_x} + f_{(p-\hat{y},p-2\hat{y})}^{\Gamma_x}}. \end{aligned} \quad (\text{S35})$$

It can be shown that, under the parameterization: $J_x = J_y = J_z = 1$, $\kappa = 0.1$, $t = 0.5$, the dual model in the zero e -particle sector will have a fermion Chern number $C = -2$.

S-IV. PROPERTIES OF ANYONS IN KITAEV MODEL

As we can see, \tilde{H} commutes with the e particle parity at each vertex and $Z_{1,2}$ of the WLS. Therefore, when it acts on a product state with a fixed configuration of $\{n_i^e\}$ and $z_{1,2}$, there is

$$\begin{aligned} \tilde{H}|\{n_i^e\}\rangle \otimes |\Psi_\varepsilon\rangle \otimes |z_1, z_2\rangle \\ = |\{n_i^e\}\rangle \otimes H_\varepsilon(\{n_i^e\}, z_1, z_2)|\Psi_\varepsilon\rangle \otimes |z_1, z_2\rangle, \end{aligned} \quad (\text{S36})$$

$\{n_i^e\}$ and $z_{1,2}$ would enter as parameters in the fermionic Hamiltonian H_ε , and the problem thus reduces to diagonalizing a purely fermionic BdG Hamiltonian. Remember that the dual space of the original spin system is the even e/ε particle number subspace of the dual space, we therefore take into account only configurations with even-parity $\{n_i^e\}$ configurations and even-parity eigenstates of $H_\varepsilon(\{n_i^e\}, z_1, z_2)$.

S-IV.A. Ground state degeneracy of the Kitaev model

The ground state of \tilde{H} should contain no e -particles, i.e., $n_i^e = 0$. $\{z_1, z_2\}$ determine the BC of the effective fermionic Hamiltonian H_ε . We can look for the lowest energy *physical* states for each case. Here we mainly focus on the so-called

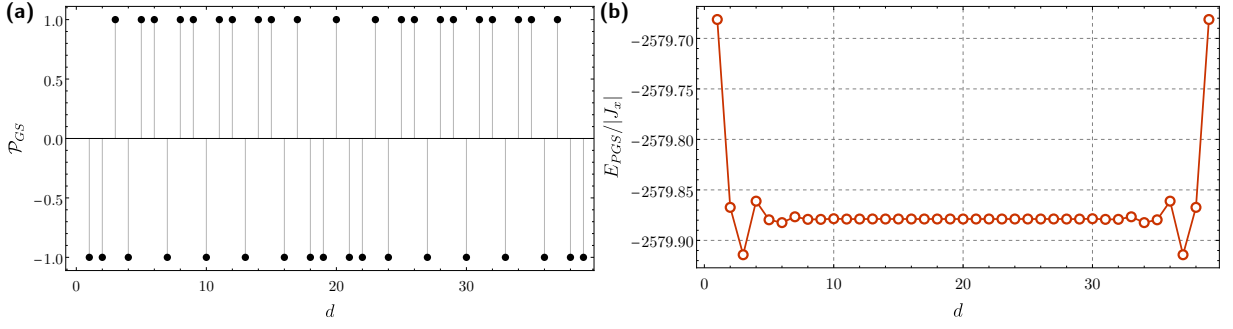


FIG. S8. Ground state parity and physical ground state energy as we move one e particle away from the other one, the WSLs are in $|-1, -1\rangle$ configuration. Parameterization: $J_x = J_y = J_z = 1$, $\kappa = 0.1$, $t = 0$, $N = 40$. (a) The ground state parity of the H_ε . The oscillation behavior of \mathcal{P}_{GS} is consistent with the fact that the coupling between the two Majorana “zero” modes is oscillating as the distance between the two e particles (vortex of the p -wave superconductor) is changing [2]. As a result, the occupation of the “zero” fermion mode is also fluctuating between 0 and 1, and leads to an oscillation of the \mathcal{P}_{GS} . However, when $\mathcal{P}_{GS} = -1$, in the lowest energy physical (even fermion parity) state, the “zero” fermion mode is still empty. Therefore, as the two e particles are separated from each other, the lowest energy physical eigenstate is always free from zero mode fermion. (b) The energy of lowest energy physical eigenstate (physical ground state) as the two e particles are separated from each other. It is clear that the energy saturate as they are away from each other, therefore support a deconfinement of the e particles.

B -phase of the Kitaev model, which is known to host gapless (fermionic) excitations without the Haldane term, and with the inclusion of Haldane term, it has a 3-fold ground state degeneracy. In this study, we will set $J_x = J_y = J_z = 1$. From our calculation, we found that for anti-periodic boundary conditions (APBC) with $(z_1, z_2) = (1, -1)$, $(-1, 1)$ or $(-1, -1)$, all the three ground states of $H_\varepsilon(n_i^e = 0, z_1, z_2)$ have an even parity and are degenerate. On the other hand, for periodic boundary condition (PBC) with $(z_1, z_2) = (1, 1)$, the ground state of $H_\varepsilon(\{n_i^e = 0\}, 1, 1)$ has an odd parity, which is *unphysical*. Therefore, the lowest energy physical eigenstate with PBC is actually the first excited state of $H_\varepsilon(\{n_i^e = 0\}, 1, 1)$ where the lowest energy Bogoliubov quasiparticle mode is occupied, and its energy is higher than that of the other three ground states of APBC. So our theory predicts the spin model’s ground state degeneracy is 3, consistent with what is expected.

S-IV.B. Deconfinement of e particles and fluctuation of fermionic ground state parity

We can study the confinement property of e particles by separating 2 of them apart and see how the physical fermionic ground state (for each e particle configuration) energy evolves during this process. In our study, with a specific WLS configuration $|z_1, z_2\rangle$ (which leads to a fixed BC for H_ε), we fix one of the e particles at the left end of some row (denote this vertex as v_0), and move the other e particle within the same row (its position is denoted as v), then calculate the fermionic ground state of $H_\varepsilon(\{n_{v_0}^e = 1, n_v^e = 1\}, z_1, z_2)$.

In our numerical calculation, we choose $(z_1, z_2) = (-1, -1)$, $\kappa = 0.1$. First of all, we check the fermionic ground state parity of $H_\varepsilon(\{n_{v_0}^e = 1, n_v^e = 1\}, z_1, z_2)$ as we vary v . It is found that the fermionic ground state parity oscillates as a function of the distance between the e particles, this fact has also been noticed in previous theoretical studies on the flux movement in a p -wave superconductor [2]. Since we are only interested in the physical ground state, when the ground state parity of H_ε is -1 , we should consider the first excited state of H_ε , and compare the energy of all the physical ground states. Fig. S8(b) shows the physical ground state energy as we move one of the e particle away from the other one in the same row. As the distance between the two e particles increases, the physical ground state energy increases and saturates to some fixed value, which indicates a deconfinement of the e particles. Note that we are considering a periodic lattice, when v is approaching the right end, the 2 particles are getting closer to each other again, thus the energy decreases in that regime.

S-IV.C. Berry phase for a single e particle around a plaquette

We also study the Berry phase for a single e particle when it moves around a single plaquette. In this case, we consider two e particles well separated from each other and fix the position of one of them at v_0 (see Fig.1 in the main text). Initially, the mobile e -particle sits at vertex 1, we can then calculate the lowest energy *physical* eigenstate of $H_\varepsilon(\{n_{v_0}^e = n_1^e = 1\}, z_1, z_2)$: $|\Psi_1^\varepsilon\rangle$. The corresponding eigenstate of \tilde{H} is $b_{v_0}^\dagger b_1^\dagger |0\rangle \otimes |\Psi_1^\varepsilon\rangle \otimes |z_1, z_2\rangle$. In the Hilbert

space of the original spin system, there is a spin state $|\Phi_1\rangle \leftrightarrow b_{s_0}^\dagger b_{s_1}^\dagger |0\rangle \otimes |\Psi_1^\varepsilon\rangle \otimes |z_1, z_2\rangle$. From the perspective of the spin system, we can then act $Z_{1,2}$ on top of $|\Phi_1\rangle$, and there is

$$Z_{1,2}|\Phi_1\rangle \leftrightarrow b_{v_0}^\dagger b_2^\dagger |0\rangle \otimes |\Psi_1^\varepsilon\rangle \otimes |z_1, z_2\rangle. \quad (\text{S37})$$

Recall that the dual operator of Z_{s_1, s_2} is: $(b_1 + b_1^\dagger)(b_2 + b_2^\dagger)$. In the meanwhile, in the sector of two e particles located at vertices v_0 and 2 (and WLS still in $|z_1, z_2\rangle$), the physical lowest energy state of \tilde{H} reads: $b_{v_0}^\dagger b_1^\dagger \otimes |\Psi_2^\varepsilon\rangle \otimes |z_1, z_2\rangle$, which is the dual state of a spin state $|\Phi_2\rangle$. Here $|\Psi_2\rangle$ is the lowest energy physical eigenstate of $H_\varepsilon(\{n_{v_0}^\varepsilon = n_2^\varepsilon = 1\}, z_1, z_2)$. The Berry phase associated with moving a single e particle from vertex 1 to 2 is:

$$\langle \Phi_2 | Z_{1,2} | \Phi_1 \rangle = \langle \Psi_2^\varepsilon | \Psi_1^\varepsilon \rangle. \quad (\text{S38})$$

Similarly, when the 2 e particles are located at $(v_0, 3)$ and $(v_0, 4)$, there are also corresponding lowest energy physical eigenstate of \tilde{H} :

$$|\Phi_{3,4}\rangle \leftrightarrow b_{v_0}^\dagger b_{3,4}^\dagger |0\rangle \otimes |\Psi_{3,4}^\varepsilon\rangle \otimes |z_1, z_2\rangle. \quad (\text{S39})$$

Here $|\Phi_{3,4}\rangle$ is the dual state in the physical spin Hilbert space, $|\Psi_{3,4}\rangle$ is the lowest energy physical eigenstate of $H_\varepsilon(\{n_{v_0}^\varepsilon = n_{3,4}^\varepsilon = 1\}, z_1, z_2)$.

Finally, the Berry phase associated moving one of the e particles around the entire plaquette is (in the original spin space):

$$e^{i\phi} = \langle \Phi_1 | Z_{4,1} | \Phi_4 \rangle \langle \Phi_4 | Z_{4,3} | \Phi_3 \rangle \langle \Phi_3 | Z_{3,2} | \Phi_2 \rangle \langle \Phi_2 | Z_{1,2} | \Phi_1 \rangle. \quad (\text{S40})$$

Mapping it to the dual space, it is:

$$e^{i\phi} = \langle \Psi_1^\varepsilon | \prod_{p \in L(4,1)} -i\gamma_p \gamma'_p | \Psi_4^\varepsilon \rangle \langle \Psi_4^\varepsilon | \Psi_3^\varepsilon \rangle \langle \Psi_3^\varepsilon | \prod_{p \in L(3,2)} -i\gamma_p \gamma'_p | \Psi_2^\varepsilon \rangle \langle \Psi_2^\varepsilon | \Psi_1^\varepsilon \rangle. \quad (\text{S41})$$

S-IV.D. Braiding of two e particles

One important feature of topological order is that it can host anyon excitations. In Kitaev model (with $C=1$), there are the non-Abelian anyons excitations and their braiding rules are [1]:

$$R_1^{\sigma,\sigma} = e^{-i\pi/8}, \quad R_\varepsilon^{\sigma,\sigma} = e^{i3\pi/8}. \quad (\text{S42})$$

In the dual space, as e -particle parity and $Z_{1,2}^W$ of WLS are good quantum number of \tilde{H} , we can do the braiding by considering an initial state with a specific $|z_1, z_2\rangle$ and 2 e -particles at vertices v_1 and v_2 . Solving the lowest energy physical eigenstate of $H_\varepsilon(\{n_{r_1}^\varepsilon = n_{r_2}^\varepsilon = 1\}, z_1, z_2)$, one can obtain the physical ground state of \tilde{H} under this specific e -particle and WLS configuration. We then need to exchange the two e particles along a certain contour and calculate the Berry phase along this process. From the perspective of the physical spin model, we are essentially acting Z_l operators on top of the state to do the braiding. In terms of the dual space, we act the dual operator of Z_l onto the states step by step and calculate the Berry phase associated within each step. Finally one can obtain the Berry phase for the entire process. The calculation is of the same type as the single-plaquette movement discussed above.

It should be noted that, in general, besides the statistical phase between anyons, the Berry phase obtained in this procedure might also contain a *geometric* phase which depends on the shape of the path. In order to get rid of this “irrelevant” geometric phase, we take the braiding path used in Ref. [1, 3, 4] (see Fig. 10 in Ref. [1]).

With $J_x = J_z = 1, \kappa = 0.1$, we found that when $J_y = 1, \phi = -\pi/8$ with APBC, and for PBC, $\phi = 3\pi/8$; when $J_y = -1: \phi = \pi/8$ with APBC, and for PBC, $\phi = -3\pi/8$. The results are consistent with the theoretical prediction discussed in Ref. [1].

For the case with $C = -2$, there are two types of anyons, which are denoted as a and \bar{a} in Ref. [1]. In order to distinguish the two types of anyons, we add an on-site energy to the 4 fermions surrounding each one of the two e particles. The on-site energies felt by the fermions are opposite between the 2 e particles. In this way, we can explore the braiding between a and \bar{a} , note that since they are different anyons, we need to do a double-exchange to get the phase. In our calculation, we found the double-exchange phase is equal to $\pi/2$, therefore the exchange phase is $\pi/4$.

S-V. BCS ANSATZ WITHOUT TRANSLATION INVARIANCE

In our study, since the dual Hamiltonian \tilde{H}_0 can be reduced to a BdG Hamiltonian with static background π fluxes (and BC (z_1, z_2)), we need to solve a BdG Hamiltonian without translational symmetry. In this section, we briefly review how one in general solves the BdG mean-field Hamiltonian without a translation symmetry. We then construct the ground state wave-function in terms of spinless fermion annihilation operators c_i defined on each (dual) lattice vertex i .

The BdG Hamiltonian is defined on a finite lattice with N sites as:

$$H = \frac{1}{2} \Psi^\dagger h_{\text{BdG}} \Psi, \quad (\text{S43a})$$

$$h_{\text{BdG}} = \begin{pmatrix} \Xi & \Delta \\ \Delta^\dagger & -\Xi^T \end{pmatrix}. \quad (\text{S43b})$$

Here $\Psi = (c_1, \dots, c_N, c_1^\dagger, \dots, c_N^\dagger)^T$. The single-particle hopping matrix Ξ satisfies the hermicity condition: $\Xi^\dagger = \Xi$, while the pairing matrix is anti-symmetric $\Delta^T = -\Delta$.

Eq. (S43) can be diagonalized into the following form:

$$\begin{aligned} H &= \frac{1}{2} \tilde{\Psi}^\dagger h_0 \tilde{\Psi} \\ &= \sum_{n=1}^N E_n \left(\alpha_n^\dagger \alpha_n - \frac{1}{2} \right). \end{aligned} \quad (\text{S44})$$

Here $h_0 = \text{diag}\{E_1, E_2, \dots, -E_1, -E_2, \dots\}$ contains the eigenvalues of h_{BdG} . $\tilde{\Psi} = (\alpha_1, \dots, \alpha_1^\dagger, \dots)^T$, where α_n annihilates a Bogoliubov quasiparticle with energy $E_n \geq 0$. It is related to c_i by a standard Bogoliubov transformation:

$$\alpha_n = \sum_i \left[u_{in}^* c_i + v_{in}^* c_i^\dagger \right]. \quad (\text{S45})$$

To find the coefficients u_{in} , v_{in}^* and energies E_n , we use the equation of motion for α_n^\dagger : $[H, \alpha_n^\dagger] = E_n \alpha_n^\dagger$, and substitute Eqs. (S43) and (S45). This gives the following eigenvalue problem for the eigenvector $C_n = (u_{1n}, \dots, u_{Nn}, v_{1n}, \dots, v_{Nn})^T$:

$$h_{\text{BdG}} C_n = E_n C_n. \quad (\text{S46})$$

The energies E_n and u_{in} , v_{in} can then be found from Eq. (S46) by exact diagonalization. Due to particle-hole symmetry of h_{BdG} , it can be shown that, for each eigenvector C_n , there exists another eigenvector $C'_n = [v_{1n}^*, \dots, v_{Nn}^*, u_{1n}^*, \dots, u_{Nn}^*]^T$ such that:

$$h_{\text{BdG}} C'_n = -E_n C'_n. \quad (\text{S47})$$

According to Eqs. (S46) and (S47), one can obtain the following relations due to orthogonality of eigenvectors:

$$\sum_i \left[u_{in}^* u_{im} + v_{in}^* v_{im} \right] = \delta_{nm}, \quad (\text{S48a})$$

$$\sum_n \left[u_{in} u_{jn}^* + v_{in}^* v_{jn} \right] = \delta_{ij}, \quad (\text{S48b})$$

$$\sum_i \left[u_{in} v_{im} + v_{in} u_{im} \right] = 0, \quad (\text{S48c})$$

$$\sum_n \left[u_{in} v_{jn}^* + v_{in}^* u_{jn} \right] = 0. \quad (\text{S48d})$$

We can now construct a ground-state wave-function of H_{BdG} taking u_{in} , v_{in} as input. As is well-known, the superconducting ground state of Eq. (S43) is a condensation of Cooper-pairs of fermions. In systems with translational

invariance, the pairing occurs between fermions with opposite momenta $\pm \mathbf{k}$ and the ground state wave-function can be written as:

$$\begin{aligned} |\Omega\rangle &= \prod_{\mathbf{k}} \left[u^*(\mathbf{k}) - v^*(\mathbf{k}) c_{\mathbf{k}}^\dagger c_{-\mathbf{k}}^\dagger \right] |0\rangle \\ &= \mathcal{N} \exp \left[\frac{1}{2} \sum_{\mathbf{k}} f(\mathbf{k}) c_{\mathbf{k}}^\dagger c_{-\mathbf{k}}^\dagger \right] |0\rangle, \end{aligned} \quad (\text{S49})$$

where $\mathcal{N} = \prod_{\mathbf{k}} u^*(\mathbf{k})$ is a normalization constant, $f(\mathbf{k}) = -f(-\mathbf{k}) = -v^*(\mathbf{k})/u^*(\mathbf{k})$, and $|0\rangle$ is the fermion vacuum state. For a system without translation invariance, we can write the ground state as:

$$|\Omega\rangle = \mathcal{N} \exp \left(\frac{1}{2} \sum_{i,j} f_{ij} c_i^\dagger c_j^\dagger \right) |0\rangle, \quad f_{ij} = -f_{ji}. \quad (\text{S50})$$

The summation in the exponent is taken over lattice sites. Note that the ground state ansatz Eq. (S50) has an even fermion parity. This may not be true in certain topologically non-trivial phases whose ground states have an odd parity, so in the context of our dual BFS space, these states are unphysical and will not be used throughout the calculation. However, as will be shown in Sec. S-VS-V.A, the first excited state, which is *physical*, can still be described by a pairing ansatz of the form in Eq. (S50).

To express f_{ij} in terms of u_{in} and v_{in} , we use the identity for the ground state:

$$\alpha_n |\Omega\rangle = 0, \quad (\text{S51})$$

and substitute Eqs. (S45) and (S50). In subsequent calculations, we bring the c_i term in Eq. (S45) to the right of the exponential in Eq. (S50). This can be done by expanding the exponential function and using the identity:

$$\left[c_i, \frac{1}{2} \sum_{j,k} f_{jk} c_j^\dagger c_k^\dagger \right] = \sum_k f_{ik} c_k^\dagger. \quad (\text{S52})$$

After some algebra, this gives for f_{ij} :

$$\sum_i f_{ij} u_{in}^* = -v_{jn}^*. \quad (\text{S53})$$

It can be shown that f_{ij} is indeed anti-symmetric. For this purpose we multiply Eq. (S53) by v_{kn} and sum over n . Substituting the orthogonality conditions Eq. (S48) then gives:

$$\sum_j f_{ij} u_{jn}^* = v_{in}^*, \quad (\text{S54})$$

which proves our statement. In what follows, we shall represent u_{in} and v_{in} as $N \times N$ matrices and write f_{ij} in matrix notation as:

$$f = v^* (u^*)^{-1}. \quad (\text{S55})$$

Eq. (S55) determines f_{ij} in terms of u_{in} and v_{in} obtained from exact diagonalization.

The normalization constant \mathcal{N} can be determined by directly computing $\langle \Omega | \Omega \rangle$. As will be discussed in Append. S-VI, there is:

$$\mathcal{N} = [\det(1 + f^\dagger f)]^{-1/4}. \quad (\text{S56})$$

Finally, we comment on a subtlety in exact diagonalization on a finite lattice. In Eq. (S50), the ‘vacuum’ state $|0\rangle$ into which the Cooper-pairs condense contains no fermions. However, this can be a bad reference state in some cases. Mathematically, this means the matrix u is not invertible and f in Eq. (S55) becomes ill-defined. For example, consider a Hamiltonian whose ground state is an atomic insulator:

$$H = -\Delta \sum_i c_i^\dagger c_i, \quad \Delta > 0. \quad (\text{S57})$$

In its ground state, every site is occupied:

$$|0\rangle_h = \prod_i^N c_i^\dagger |0\rangle. \quad (\text{S58})$$

If one tries to express $|0\rangle_h$ using the BCS ansatz in momentum space in Eq. (S59), it would correspond to the limit $u(\mathbf{k}) = 0$, and $f(\mathbf{k}) \rightarrow \infty$ as a result. For ground states sufficiently close to $|0\rangle_h$, the matrix u might not be invertible numerically. This problem can be avoided by choosing Eq. (S58) as the new ‘vacuum’ state and consider a condensation of hole pairs on top of it. Thus the BCS Ansatz in this case is:

$$|\Omega\rangle = \mathcal{N} \exp\left(\frac{1}{2} \sum_{i,j} g_{ij} c_i c_j\right) |0\rangle_h. \quad (\text{S59})$$

It can be shown that the (hole) Cooper wave function $g_{ij} = u^*(v^*)^{-1}$.

S-V.A. The first excited state of a BdG Hamiltonian having an odd ground state parity

As discussed in the previous section, in certain topologically non-trivial phases, the ground state of a BdG Hamiltonian has an odd fermion parity. These states are unphysical does not belong to the dual space of a periodic spin system. Therefore, the lowest energy physical eigenstate of H_{BdG} will be the first excited state $|\Psi_1\rangle = \alpha_1^\dagger |\Psi_0\rangle$. In this section, we show that $|\Psi_1\rangle$ can be also expressed by an ansatz of the form in Eq. (S50).

By definition, $|\Psi_1\rangle$ satisfies:

$$\alpha_1^\dagger \alpha_1 |\Psi_1\rangle = |\Psi_1\rangle; \quad \alpha_n |\Psi_1\rangle = 0, \quad n \neq 1. \quad (\text{S60})$$

$\alpha_n, \alpha_n^\dagger$ are given in Eq. (S44). For our purpose, it is more convenient to consider another Hamiltonian:

$$H' = \sum_{n=2}^N E_n \left(\alpha_n^\dagger \alpha_n - \frac{1}{2} \right) - E_1 \left(\alpha_1^\dagger \alpha_1 - \frac{1}{2} \right), \quad (\text{S61})$$

for which $|\Psi_1\rangle$ is the ground state. Obviously, there is:

$$\begin{aligned} H' &= \frac{1}{2} \tilde{\Psi}^\dagger h'_0 \tilde{\Psi}, \\ &= \frac{1}{2} \Psi^\dagger h'_{\text{BdG}} \Psi. \end{aligned} \quad (\text{S62})$$

where $h'_0 = \text{diag}\{-E_1, E_2, \dots, E_N, E_1, -E_2, \dots, -E_N\}$, which is related to the h_0 through a permutation P :

$$h'_0 = P h_0 P. \quad (\text{S63})$$

Here $P_{ii} = 1$ for $i \neq 1, N+1$, $P_{1,N+1} = P_{N+1,1} = 1$ and zero otherwise. Using the fact that

$$\begin{aligned} \Psi &= U \tilde{\Psi}, \\ U &= \begin{pmatrix} u & v^* \\ v & u^* \end{pmatrix}, \end{aligned} \quad (\text{S64})$$

one can obtain:

$$\begin{aligned} h'_{\text{BdG}} &= U P h_0 P U^\dagger \\ &= \tilde{U} h_0 \tilde{U}^\dagger, \end{aligned} \quad (\text{S65})$$

with

$$\tilde{U} = U P \equiv \begin{pmatrix} \tilde{u} & \tilde{v}^* \\ \tilde{v} & \tilde{u}^* \end{pmatrix}. \quad (\text{S66})$$

Using the ansatz

$$|\Psi_1\rangle = \mathcal{N} \exp\left(\frac{1}{2} \sum_{i,j} \tilde{f}_{ij} c_i^\dagger c_j^\dagger\right) |0\rangle, \quad (\text{S67})$$

it can be shown that $\tilde{f} = \tilde{v}^*(\tilde{u}^*)^{-1}$.

S-VI. OVERLAP BETWEEN BCS STATES

In this paper, we compute matrix elements and overlaps of ground states of BdG Hamiltonians with different e particle configurations. Since e particles act as a π -flux for fermions, each configuration of e corresponds to a different set of matrix elements Ξ , Δ in Eq. (S43). Therefore, we consider two such BCS ground states:

$$|\Omega_0\rangle = \mathcal{N}_0 |\tilde{\Omega}_0\rangle = \mathcal{N}_0 \exp\left(\frac{1}{2} \sum_{i,j} f_{i,j}^{(0)} c_i^\dagger c_j^\dagger\right) |0\rangle, \quad (\text{S68a})$$

$$|\Omega_1\rangle = \mathcal{N}_1 |\tilde{\Omega}_1\rangle = \mathcal{N}_1 \exp\left(\frac{1}{2} \sum_{i,j} f_{i,j}^{(1)} c_i^\dagger c_j^\dagger\right) |0\rangle. \quad (\text{S68b})$$

$\mathcal{N}_{0,1}$ are defined in Eq. (S56), and $f^{(1)}$, $f^{(2)}$ are given by exact diagonalization of the respective Hamiltonians; see Eq. (S55). The overlap between the two states have been calculated, for example in Ref. [5] using the fermion coherent-state integral method:

$$\langle \tilde{\Omega}_0 | \tilde{\Omega}_1 \rangle = (-1)^{\frac{N(N+1)}{2}} \text{pf} \left[\begin{pmatrix} f^{(1)} & -I \\ I & f^{(0)\dagger} \end{pmatrix} \right]. \quad (\text{S69})$$

$\text{pf}(A)$ is the Pfaffian of matrix A . In particular, by taking $|\tilde{\Omega}_0\rangle = |\tilde{\Omega}_1\rangle$, we arrive at Eq. (S56) for the normalization constant \mathcal{N} .

The matrix elements of products of fermion parity operators $\prod_p G_p = \exp(-i\pi \sum_p c_p^\dagger c_p)$ between two BCS ground states can be expressed in a similar form to Eq. (S69). For simplicity, we first consider the matrix element on a single plaquette p :

$$\langle \Omega_1 | G_p | \Omega_0 \rangle = \mathcal{N}_1 \mathcal{N}_0 \langle 0 | \exp\left(\frac{1}{2} \sum_{i,j} f_{i,j}^{(1)*} c_j c_i\right) G_p \exp\left(\frac{1}{2} \sum_{i,j} f_{i,j}^{(0)} c_i^\dagger c_j^\dagger\right) | 0 \rangle. \quad (\text{S70})$$

In Eq. (S70) we insert on the RHS the identity $G_p^2 = 1$:

$$\mathcal{N}_1 \mathcal{N}_0 \langle 0 | \exp\left(\frac{1}{2} \sum_{i,j} f_{i,j}^{(1)*} c_j c_i\right) G_p \exp\left(\frac{1}{2} \sum_{i,j} f_{i,j}^{(0)} c_i^\dagger c_j^\dagger\right) G_p | 0 \rangle. \quad (\text{S71})$$

To evaluate the matrix exponential, we use the following identity (remember that G_p is hermitian):

$$G_p c_i^\dagger G_p = e^{i\pi c_p^\dagger c_p} c_i^\dagger e^{-i\pi c_p^\dagger c_p} = c_i^\dagger \exp(i\pi \delta_{ip}) = (-1)^{\delta_{ip}} c_i^\dagger. \quad (\text{S72})$$

Eq. (S72) can be obtained by noting that $\exp(-i\pi c_p^\dagger c_p)$ is formally a single-particle time evolution operator with energy $\varepsilon_p = 1$ and time $t = \pi$, and $c_p^\dagger \rightarrow c_p^\dagger \exp(i\varepsilon_p t)$ under such a transformation. From Eq. (S72) and that $G_p | 0 \rangle = | 0 \rangle$, Eq. (S71) becomes:

$$\mathcal{N}_1 \mathcal{N}_0 \langle 0 | \exp\left(\frac{1}{2} \sum_{i,j} f_{i,j}^{(1)*} c_j c_i\right) \exp\left(\frac{1}{2} \sum_{i,j} \tilde{f}_{i,j}^{(0)} c_i^\dagger c_j^\dagger\right) | 0 \rangle; \quad \tilde{f}_{ij} = (-1)^{\delta_{ip}} f_{ij} (-1)^{\delta_{jp}}. \quad (\text{S73})$$

Above can be immediately generalized to matrix elements of a product of fermion parity operators:

$$\langle \Omega_1 | \prod_p G_p | \Omega_0 \rangle = \mathcal{N}_1 \mathcal{N}_0 \langle 0 | \exp\left(\frac{1}{2} \sum_{i,j} f_{i,j}^{(1)*} c_j c_i\right) \exp\left(\frac{1}{2} \sum_{i,j} \tilde{f}_{i,j}^{(0)} c_i^\dagger c_j^\dagger\right) | 0 \rangle. \quad (\text{S74})$$

Now \tilde{f}_{ij} satisfies:

$$\tilde{f}_{ij} = (-1)^{\sum_p \delta_{ip}} f_{ij} (-1)^{\sum_p \delta_{jp}}, \quad (\text{S75})$$

where the summation is taken over the plaquettes of the fermion parity operators. In matrix notation, Eq. (S75) can be written as:

$$\tilde{f} = \left(\prod_p I_p \right) f \left(\prod_p I_p \right), \quad (\text{S76})$$

where $(I_p)_{ij} = \delta_{ij}(-1)^{\delta_{ip}}$ is a diagonal matrix with elements unity apart from the p -th diagonal, which has element -1 . Eqs. (S74), (S75) together with Eqs. (S69) and (S56) determine the matrix elements of fermion parities.

-
- [1] A. Kitaev, Anyons in an exactly solved model and beyond, [Ann. Phys. **321**, 2 \(2006\)](#).
 - [2] M. Cheng, R. M. Lutchyn, V. Galitski, and S. Das Sarma, Tunneling of anyonic majorana excitations in topological superconductors, [Phys. Rev. B **82**, 094504 \(2010\)](#).
 - [3] M. Levin and X.-G. Wen, Fermions, strings, and gauge fields in lattice spin models, [Phys. Rev. B **67**, 245316 \(2003\)](#).
 - [4] K. Kawagoe and M. Levin, Microscopic definitions of anyon data, [Phys. Rev. B **101**, 115113 \(2020\)](#).
 - [5] L. M. Robledo, Sign of the overlap of hartree-fock-bogoliubov wave functions, [Phys. Rev. C **79**, 021302 \(2009\)](#).